Article

Current Biology

Cephalopod retinal development shows vertebrate-like mechanisms of neurogenesis

Graphical abstract

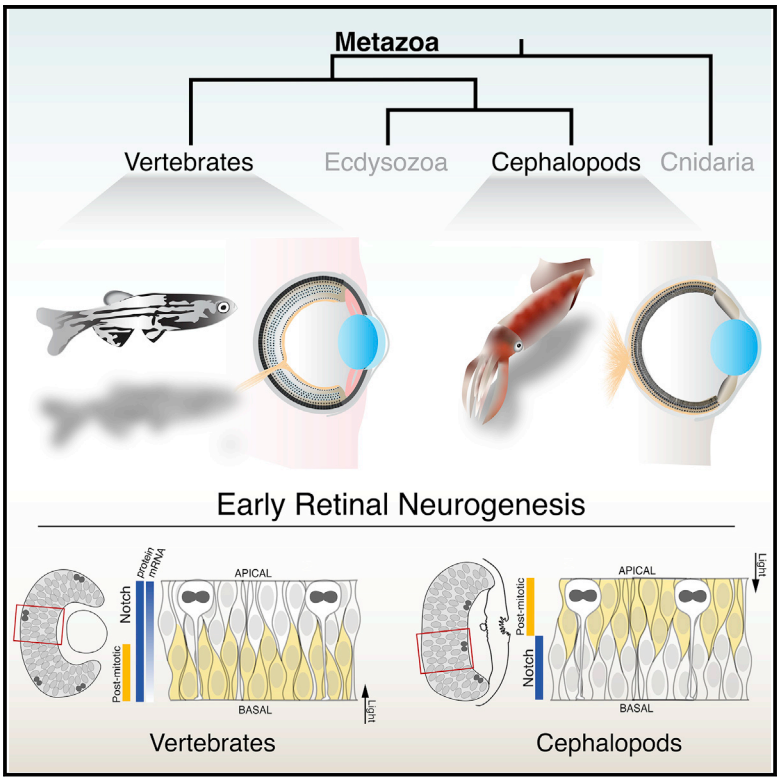

Authors

Francesca R. Napoli, Christina M. Daly, Stephanie Neal, Kyle J. McCulloch, Alexandra R. Zaloga, Alicia Liu, Kristen M. Koenig

Correspondence

kmkoenig@fas.harvard.edu

In brief

Napoli, Daly, et al. find that progenitor cells in the squid retina undergo interkinetic nuclear migration and that Notch signaling may regulate differentiation, similar to vertebrate processes. These results reveal the convergent evolution of cellular mechanisms that underlie the growth of highly proliferative neurogenic primordia.

Highlights

- Retinal progenitor cells in the squid undergo interkinetic nuclear migration
- Progenitor, post-mitotic, and differentiated cells are transcriptionally defined
- Notch signaling may regulate both retinal cell cycle and cell fate in the squid

Napoli et al., 2022, Current Biology *32*, 1–12
December 5, 2022
https://doi.org/10.1016/j.cub.2022.10.027

CellPress

Please cite this article in press as: Napoli et al., Cephalopod retinal development shows vertebrate-like mechanisms of neurogenesis, Current Biology (2022), https://doi.org/10.1016/j.cub.2022.10.027

Current Biology

CellPress

Article

Cephalopod retinal development shows vertebrate-like mechanisms of neurogenesis

Francesca R. Napoli,[1,2,3] Christina M. Daly,[1,2,3] Stephanie Neal,[1,2] Kyle J. McCulloch,[1,2,4] Alexandra R. Zaloga,[1,2] Alicia Liu,[1,2] and Kristen M. Koenig[1,2,5,6,*]

[1]John Harvard Distinguished Science Fellowship Program, Harvard University, Cambridge, MA 02138, USA
[2]Department of Organismic and Evolutionary Biology, Harvard University, Harvard University, Cambridge, MA 02138, USA
[3]These authors contributed equally
[4]Present address: Department of Ecology, Evolution, and Behavior, University of Minnesota, St. Paul, MN 55108, USA
[5]Twitter: @eye_evolution
[6]Lead contact
*Correspondence: kmkoenig@fas.harvard.edu
https://doi.org/10.1016/j.cub.2022.10.027

SUMMARY

Coleoid cephalopods, including squid, cuttlefish, and octopus, have large and complex nervous systems and high-acuity, camera-type eyes. These traits are comparable only to features that are independently evolved in the vertebrate lineage. The size of animal nervous systems and the diversity of their constituent cell types is a result of the tight regulation of cellular proliferation and differentiation in development. Changes in the process of development during evolution that result in a diversity of neural cell types and variable nervous system size are not well understood. Here, we have pioneered live-imaging techniques and performed functional interrogation to show that the squid *Doryteuthis pealeii* utilizes mechanisms during retinal neurogenesis that are hallmarks of vertebrate processes. We find that retinal progenitor cells in the squid undergo nuclear migration until they exit the cell cycle. We identify retinal organization corresponding to progenitor, post-mitotic, and differentiated cells. Finally, we find that Notch signaling may regulate both retinal cell cycle and cell fate. Given the convergent evolution of elaborate visual systems in cephalopods and vertebrates, these results reveal common mechanisms that underlie the growth of highly proliferative neurogenic primordia. This work highlights mechanisms that may alter ontogenetic allometry and contribute to the evolution of complexity and growth in animal nervous systems.

INTRODUCTION

Coleoid cephalopods (e.g., squid, cuttlefish, and octopus) are charismatic invertebrates known for their expansive behavioral repertoire and large nervous systems, which have independently evolved from similar features found in vertebrate species (Figure 1A).[1,2] Although vertebrates have been well studied, the developmental changes that underlie the evolution of large, complex nervous systems are not well understood. Across animals, we know that in some cases neurogenesis is regulated through invariant numbers of precursors with fixed lineages (i.e., *C. elegans*), and in others, cell lineages are plastic and proliferation is temporally controlled (i.e., the vertebrate retina).[3–5] Live-imaging has revealed that neurodifferentiation and the regulation of growth is not only a genetic process but also a cell biological process, dictated by orchestrated cell behaviors and tissue architecture. However, *in vivo* observations of cell behavior during neurogenesis have been primarily limited to traditional model species. To elucidate how changes in neurogenesis may contribute to the evolution of large and complex nervous systems, we sought to understand neurodifferentiation in the cephalopod. One of the striking features of the cephalopod nervous system is its highly acute, camera-type eyes. The visual system has proven to be a powerful context to learn fundamental aspects of neural development and, therefore, we focused our investigations on retinal differentiation in the squid, *Doryteuthis pealeii*.

The cephalopod retina is composed of two layers, divided by the basal membrane (Figures 1B–1D). Photoreceptor cell bodies are found posterior (further from the lens) to the basal membrane and support cells are found anterior (closer to the lens). The photoreceptor cells extend projections that pierce through the basal membrane to the anterior of the retina to form the outer segment, which is a region of expanded membrane, packed with proteins required for phototransduction (Figure 1D).[20,21] This arrangement is notably inverted relative to the vertebrate retina, which has photoreceptor cells and their outer segment in the posterior (Figures 2A and S1). Cephalopod photoreceptor cells also extend axons out of the retina and synapse directly onto the optic lobe.[20,21] The function of the support cells is not well understood but thought to act as photoreceptor sustaining glial-like cell as well as a potential stem cell population for ongoing growth.[22,23] Both photoreceptors and support cells are pigmented.[6] Previous work has shown that both support

Please cite this article in press as: Napoli et al., Cephalopod retinal development shows vertebrate-like mechanisms of neurogenesis, Current Biology (2022), https://doi.org/10.1016/j.cub.2022.10.027

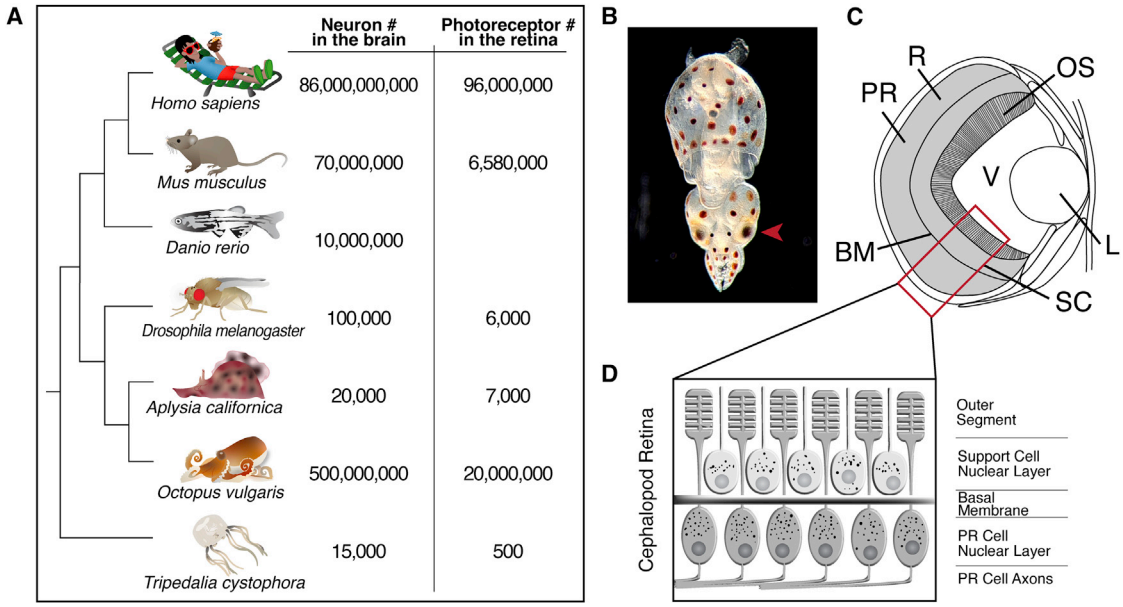

Figure 1. The evolution of nervous system complexity in the cephalopod lineage

(A) Phylogeny of animals, with approximate neuron number in the brain and photoreceptor cell number in the retina, where available. *Tripedalia cystophora*, which does not have a central nervous system, includes an average of two counts of the ring nerve as well as rhopalia neuron counts, excluding associated retinal neurons. Photoreceptor cell calculations in *Tripedalia cystophora* include all retina-associated cells in a single rhopalium.[6–18]

(B) A hatching-stage squid, *Doryteuthis pealeii* (stage 29).[19] The red arrowhead points at one of the eyes.

(C) A schematic of the hatching-stage eye of *D. pealeii*. *R*, retina; *L*, lens; *OS*, outer segment; *V*, vitreous space; *PR*, photoreceptor nuclear layer; *SC*, support cell layer; *BM*, basal membrane.

(D) Simplified schematic of photoreceptor cells and support-cell organization in the squid retina. See also Figure S1.

cells and photoreceptor cells are derived from bilateral, early-emerging retinal primordia.[23]

Previous observations from fixed tissue suggest that the cephalopod retinal primordium is a pseudostratified epithelium, which is unusual for an invertebrate neurogenic tissue (Figure 2A).[23,24] This type of neuroepithelium is characteristic of central nervous system development in vertebrates, including the retina.[25,26] A pseudostratified epithelium is a monolayer composed of elongated cells with nuclei distributed along the apicobasal axis. Cells in pseudostratified epithelia undergo nuclear movements correlated with the cell cycle called interkinetic nuclear migration.[27] During nuclear migration, mitosis occurs on the apical surface, which corresponds to the posterior side of the developing retina in vertebrates (Figure 2A).[28] Eventually, cells delaminate and differentiate within the boundaries of the epithelium. These cell behaviors are required for proper nervous system development, although their function is not completely understood.[29] Supporting the expectation that a similar mechanism may occur in the squid, fixed time point data suggest that mitosis occurs only on the apical side of the developing retina (anterior in the eye), inverted relative to vertebrates (Figures 2A and S1).[23] This inversion is a result of early epithelial morphogenesis. The vertebrate retina is the result of an invagination of the evaginated forebrain, and the squid retina is a result of the invagination of a superficial placode (Figure S1).[30] Here, we present descriptive and functional evidence that cephalopod neurogenesis shows exceptional similarity to vertebrate processes, suggesting that the deployment of common developmental mechanisms led to the evolution of convergent visual organ expansion.

RESULTS

Cell cycle in the developing squid retina

Previous work in the squid retina showed that at Arnold stage 23, a 3-h bromo-deoxyuridine (BrdU) pulse, an analog of thymidine incorporated in S phase, resulted in incorporation throughout the retina.[19,23] If nuclei are undergoing interkinetic nuclear migration, this long pulse would provide sufficient time for movement after incorporation. To more precisely understand cell-cycle state in the early retina, we performed a 10-min BrdU pulse experiment, fixed immediately, and performed immunofluorescence for phosphohistone H3 (PH3), a marker for mitosis (Figure 2B). BrdU incorporation is restricted to the posterior of the retina after 10 min. In addition, PH3-positive nuclei in late G2 and M phase are on the apical surface of the retina, supporting previous observations.[23] The substantial number of BrdU-negative nuclei in the anterior retina suggests a population of cells that are in G1, G2, or post-mitotic phase.

If cells are undergoing interkinetic nuclear migration, we expect BrdU-positive nuclei to eventually migrate apically (anterior) to divide. To test this hypothesis, we chased our 10-min BrdU pulse, sampling embryos every 10 min for 110 min, again co-labeling with PH3 (Figure 2C). At 70 min after the initial 10-min pulse, BrdU-positive, PH3-positive cells are on the apical side of the retinal epithelium, suggesting that nuclei do migrate apically (Figures 2D and 2E). If proliferative cells found on the basal side of the epithelium join a post-mitotic population on the apical side of the epithelium, we expect to find BrdU-positive, PH3-negative cells apical after mitosis. Assuming most

Please cite this article in press as: Napoli et al., Cephalopod retinal development shows vertebrate-like mechanisms of neurogenesis, Current Biology (2022), https://doi.org/10.1016/j.cub.2022.10.027

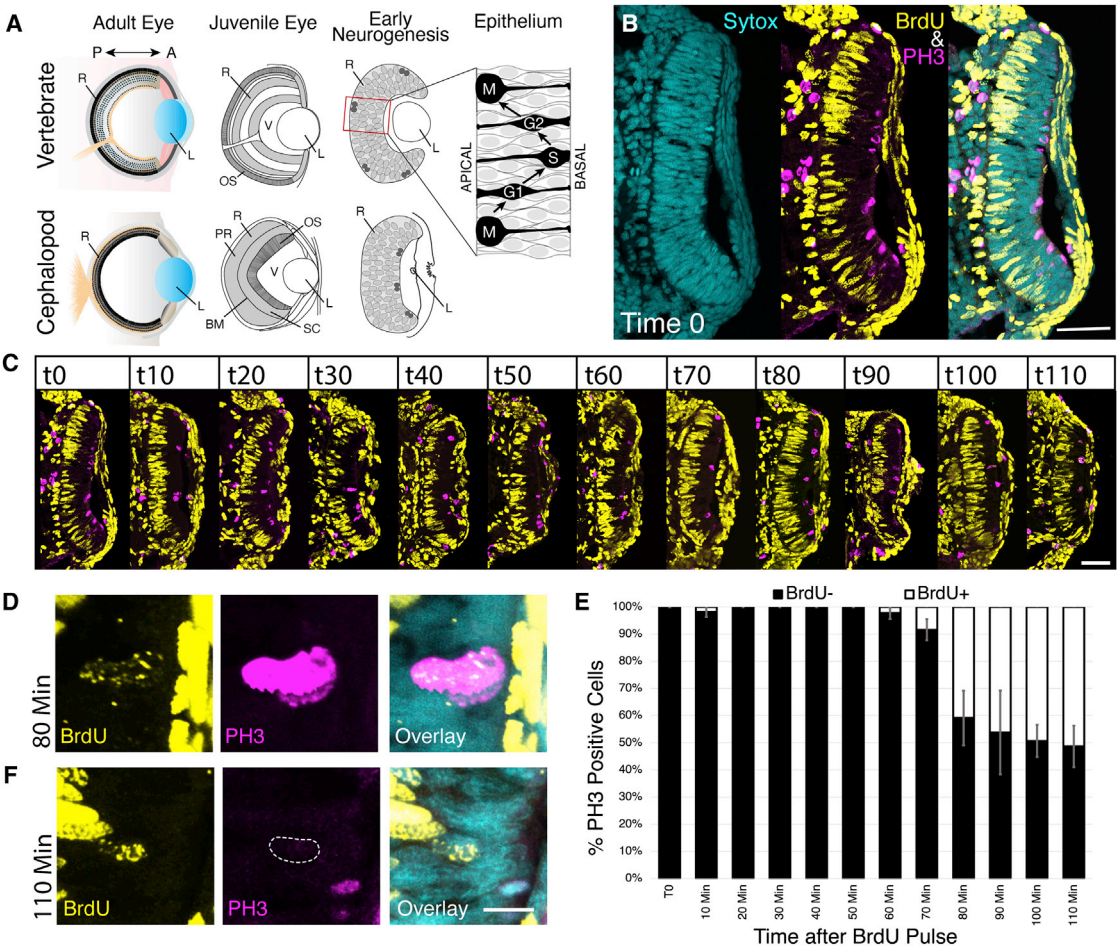

Figure 2. Growth and cell cycle during neurogenesis

(A) Schematic of the vertebrate and cephalopod eye at adult, juvenile, and early-stage development. The early neurogenesis stage is prior to when obvious organization and differentiation has occurred. Box shows enlargement of the vertebrate pseudostratified epithelium, apical to the left. Gray ovals are the nuclei distributed across the tissue early in development, darker gray nuclei are undergoing mitosis. Mitoses in the vertebrate retina are found in the posterior, and in the squid retina they are found in the anterior (the apical side of the epithelium in each instance). Squid eye schematics depict the adult eye, Arnold stages 29 and 23. *R*, retina; *L*, lens; OS, outer segment; *V*, vitreous space; *PR*, photoreceptor nuclear layer; *SC*, support cell layer; *BM*, basal membrane.

(B) 10-min BrdU pulse and immediate fix (time 0) BrdU/PH3 antibody stain shows BrdU incorporation on the basal side of the epithelium (S phase) and PH3 stain on the apical side of the epithelium (M phase). Scale bar, 50 μm.

(C) Representative images from the BrdU/PH3 time course dataset used for quantification. Scale bar, 50 μm.

(D) Example of a BrdU+/PH3+ nucleus found on the apical side of the retina, 80 min after BrdU pulse.

(E) Proportion of PH3-positive nuclei that are BrdU− and BrdU+ at 10-min time intervals after an initial 10-min BrdU pulse. SEM (standard error of the mean) is shown.

(F) Example of a BrdU+/PH3− nucleus found on the apical side of the retina at 110 min after BrdU pulse. The incidence of apical BrdU+/PH3− nuclei is low. Scale bar, 10 μm for both (D) and (F).

mitoses are not terminal, we also expect to find few BrdU-positive, PH3-negative nuclei. Indeed, at 110 min we find rare BrdU-positive, PH3-negative cells apical in the retinal epithelium (Figure 2F). Together, these data suggest that cells in the cell cycle have nuclei residing in the basal retina and that these nuclei migrate apically to divide. Some cells exit the cell cycle and their cell bodies remain anterior. These data are consistent with cells undergoing interkinetic nuclear migration. Although high resolution data describing neurogenesis across species is limited, we hypothesize that this is an ancestral developmental mechanism that has been convergently deployed in the context of neurogenesis in both cephalopods and vertebrates.

Live-imaging observations of nuclear migration in the squid retinal epithelium

To fully understand the dynamics of these cell behaviors, it is necessary to observe development *in vivo*. This required us to generate a cell-resolution, live-imaging protocol in cephalopods. We injected fluorescent Dextran to broadly label cell membranes and performed >9-h time course experiments of the squid retina at stage 23 (Figure 3A). Within these datasets, we were able to track individual nuclei migrate from the basal lamina to the apical side of the retina, mitose, and migrate basally again (Figures 3B and 3C; Videos S1–S3). These data confirm the process of interkinetic nuclear migration in the squid retina. From these data, we were able to

Please cite this article in press as: Napoli et al., Cephalopod retinal development shows vertebrate-like mechanisms of neurogenesis, Current Biology (2022), https://doi.org/10.1016/j.cub.2022.10.027

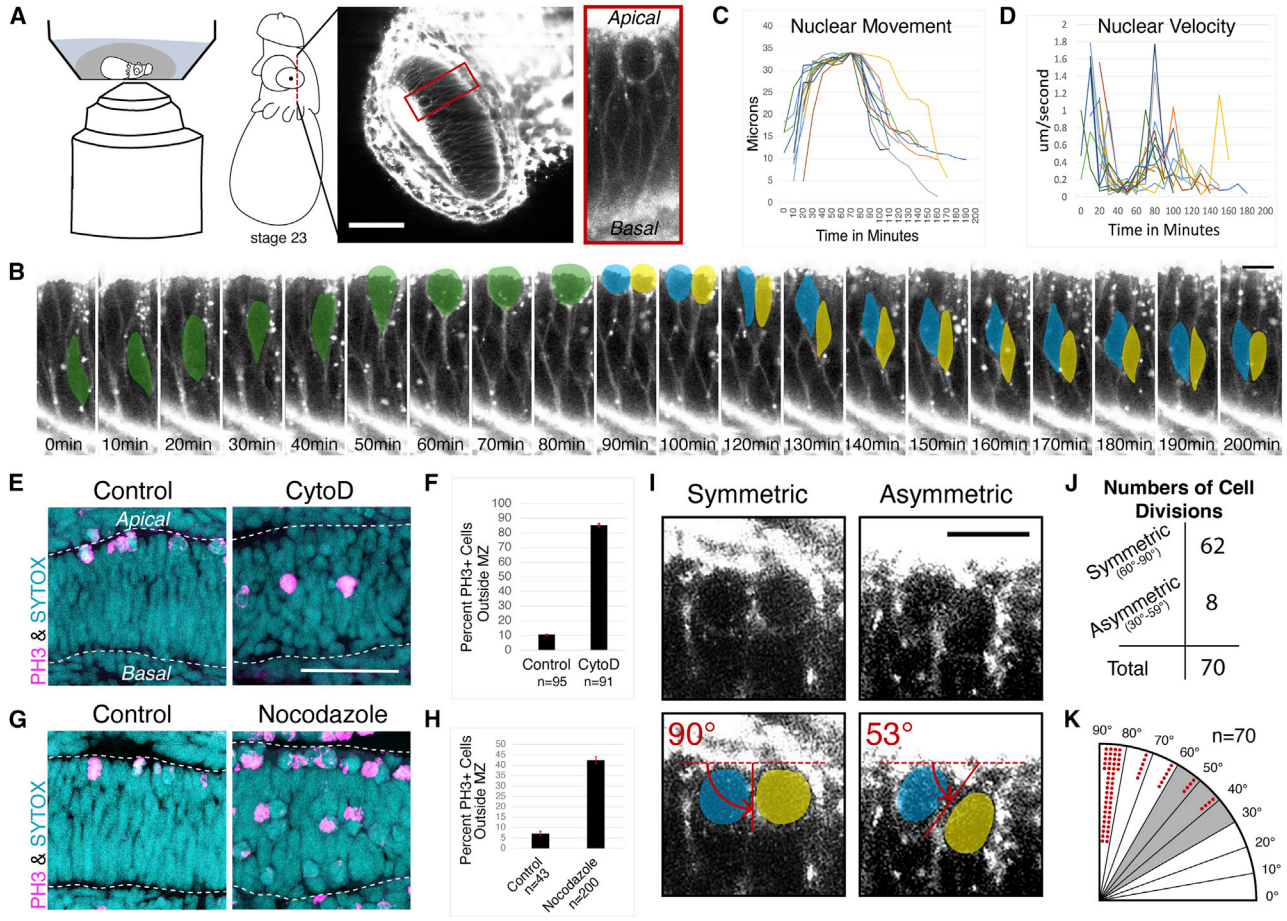

Figure 3. Live-imaging of nuclear migration and mitosis in the retinal epithelium at stage 23

(A) Schematic of squid embryo live-imaging. Scale bar is 50 μm.

(B) False-colored time-lapse of a single mitosis in the squid retina at stage 23, showing the apical migration of a nucleus in the epithelium, mitosis, and basal migration. Apical is up, basal is down. Scale bar is 10 μm.

(C) Graph of nuclear movement as tracked using the Trackmate Fiji plugin.[35] 13 nuclei tracked in 3 embryos. Tracks aligned to the highest point in migration.

(D) Graph of nuclear velocity calculated from the cells tracked in (C).

(E) PH3 immunohistochemistry on actin-polymerization-inhibited squid retina at stage 23. 5 μM cytochalasin D and DMSO control treatment for 7 h and immediate fix. We see a significant increase in cells outside the mitotic zone in our CytoD-treated embryo, suggesting that actin polymerization is required for nuclear migration. Scale bar is 50 μm.

(F) Quantification of PH3+ nuclei outside the mitotic zone.

(G) PH3 immunohistochemistry on microtubule-polymerization-inhibited squid retina at stage 23. 5 μM nocodazole and DMSO control treatment for 7 h and immediate fix. Relative to control, we find an accumulation of PH3-positive nuclei in the mitotic zone as well as a population of PH3-positive nuclei away from the mitotic zone, suggesting that microtubules do play some role in nuclear migration.

(H) Quantification of PH3+ nuclei outside of the mitotic zone.

(I) Example of symmetrical and asymmetrical cell divisions observed in live-imaging experiments. Measurement of angle of division shown. Scale bar is 10 μm.

(J) Quantification of symmetrical (60°–90°) and asymmetrical (30°–60°) cell divisions, n = 70 mitoses from videos of 5 embryos.

(K) Radial histogram quantification of division angles. Each dot represents a single mitosis. See also Videos S1–S3.

calculate distance traveled and nuclear velocity and assess that migratory behavior is quantitatively similar to movements in the vertebrate retina. The mean nuclear velocity in the zebrafish and mouse retina is approximately 0.3 μm/min (Figure 3D).[31–34]

The cytoskeletal elements contributing to nuclear migration have been interrogated in a number of developmental contexts, and their contribution has been shown to vary.[25,27,32,36,37] To understand the proteins involved in nuclear migration in the squid retina, we treated stage-23 embryos with either the actin polymerization inhibitor, cytochalasin D, or the microtubule polymerization inhibitor, nocodazole, for 7 h and fixed immediately. The impact of these inhibitors on nuclear migration was assessed using immunofluorescence for PH3 (Figures 3E–3H). In control embryos, as expected, the majority of PH3-positive nuclei are in the mitotic zone (MZ), defined as the region of the epithelium containing nuclei abutting the apical membrane. We also find a small percentage outside the mitotic zone in controls, which we hypothesize are at the end of G2, migrating toward the apical surface. Cytochalasin D- and

Please cite this article in press as: Napoli et al., Cephalopod retinal development shows vertebrate-like mechanisms of neurogenesis, Current Biology (2022), https://doi.org/10.1016/j.cub.2022.10.027

CellPress

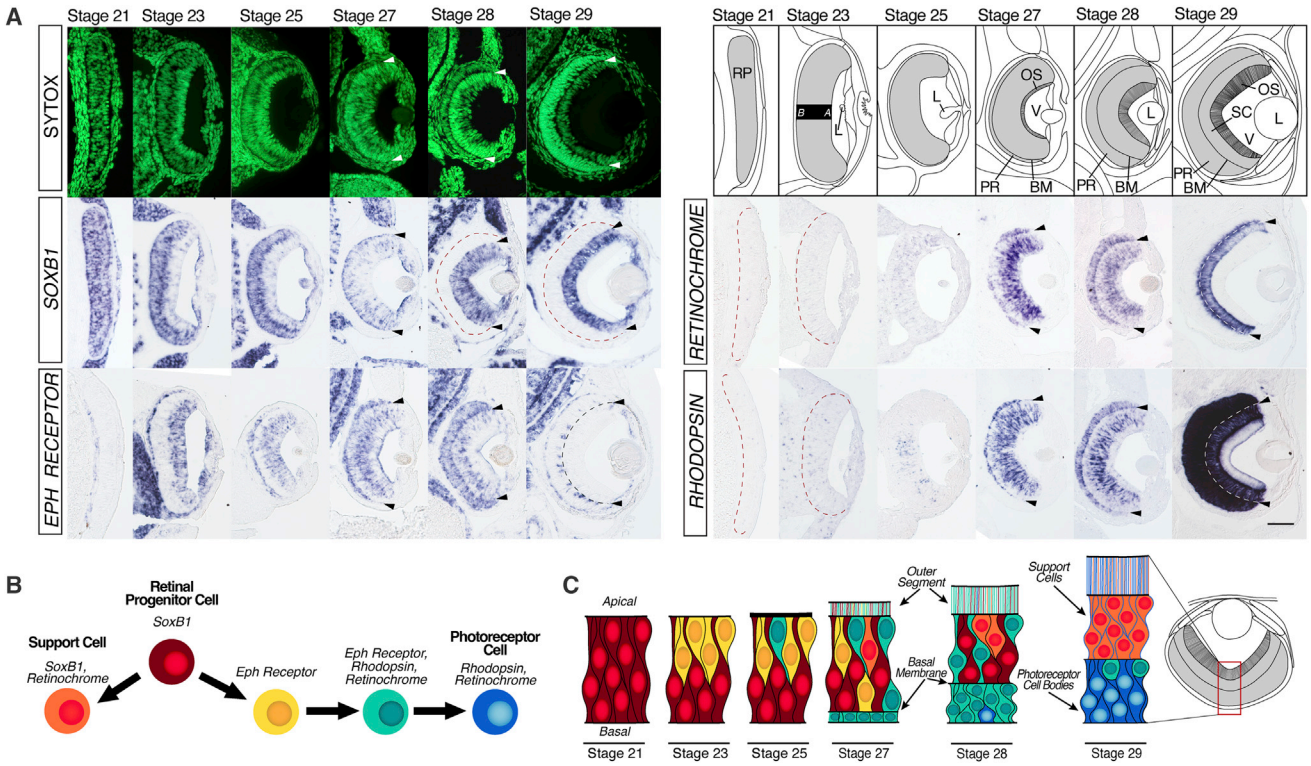

Figure 4. Molecular marker expression suggests retinal differentiation trajectories

(A) Staged mRNA expression in the developing cephalopod retina: *DpSoxB1, DpEphR, DpRhodopsin, DpRetinochrome*. Nuclear stain (SYTOX) shown in green. Schematic of stages shown. Arrowheads and black and white dotted lines identify the basal membrane. Red dotted lines identify the posterior retinal boundary. *DpSoxB1* is homogeneously expressed across the retinal epithelium at stage 21. At stage 23, *DpSoxB1* is basal and *DpEphR* is apical, correlating with BrdU-positive and BrdU-negative nuclei, respectively. At stage 25, terminal differentiation markers, *DpRhodopsin* and *DpRetinochrome*, are evident. At stage 27, the basal membrane is evident and the stage 23 and 25 mRNA segregation dissolves. mRNA segregation is re-established as *DpSoxB1* expression is never found posterior to the basal membrane and *DpEphR* is found on both sides of the membrane at stage 29. Terminal differentiation markers span both sides of the basal membrane at stage 29. Scale bar is 50 μm. *RP*, retinal placode; *L*, Lens; *OS*, outer segment; *BM*, basal membrane; *PR*, photoreceptor cells; *SC*, support cells; *V*, vitreous space; *A*, apical; *B*, basal. Stage 21, 23, and 25 embryo anterior is down. Stages 27, 28, and 29 embryo dorsal is up.

(B) Hypothesis of cell differentiation trajectories. Color key is used in (C).

(C) High magnification summary of time course gene expression data. At stage 21, the retina is homogenous. At stage 23, the retina is divided into apical and basal regions. At stage 27, the first nuclei are found behind the basal membrane and strict segregation of apical and basal expression is lost. We hypothesize that the cell bodies migrate or mix, with apical cells moving to the posterior of the retina and basal cells moving to the anterior of the retina. This resorting may move the post-mitotic cells to the posterior,where they will become the first photoreceptor cell bodies to migrate behind the basal membrane. At stage 28, the number of photoreceptor cells behind the basal membrane has increased and gene expression shows increased regional segregation. At stage 29, differentiation markers are robustly expressed. See also Figures S2 and S3 and Table S1.

nocodazole-treated retinas have PH3-positive nuclei displaced from the mitotic zone, suggesting that both actin and microtubule polymerization are required for nuclear migration (Figures 3E–3H). We also find an accumulation of arrested mitotic nuclei at the apical surface after nocodazole treatment, which has been previously observed when microtubules are not required for nuclear migration.[38] These data suggest heterogeneity in the cytoskeletal mechanism required for nuclear movement.

In addition to nuclear movement, we were also able to assess the angle of cell division in the epithelium relative to the apical surface. The plane of cell division that is 60°–90° relative to the apical surface is considered symmetric, while 0°–60° is considered asymmetric.[39,40] Symmetrical and asymmetrical cell division is an essential aspect of regulating self-renewal, delamination, cell-cycle exit, and cell fate commitment during neurogenesis in multiple organisms.[41–43] This phenomenon is variable across bilaterian species and neurodevelopmental contexts, inside and outside pseudostratified epithelia, and has been previously reviewed.[3] However, when angled cell divisions are observed, symmetrical divisions are commonly self-renewing. Most mitoses observed at stage 23 in the squid retina were symmetrical, defined by having a division plane angle between 60° and 90° relative to the apical surface (Figure 3I; Video S2). We hypothesize that these divisions are self-renewing. Approximately 10% of cell divisions are asymmetric, angled 30°–60° relative to the apical surface (Figures 3I, 3J, and 3K; Video S3). We hypothesize that these asymmetrical cell divisions may contribute to cells exiting the cell cycle. We did not observe cell divisions perpendicular to the apical surface, (0°–30°) as observed in other systems.[39,40]

Molecular identity during retinal neurogenesis

To better understand the molecular state correlated with cell-cycle organization observed in our BrdU and live-imaging

Please cite this article in press as: Napoli et al., Cephalopod retinal development shows vertebrate-like mechanisms of neurogenesis, Current Biology (2022), https://doi.org/10.1016/j.cub.2022.10.027

experiments, we sought to identify markers that define differentiation trajectories in the cephalopod retina. We analyzed spatiotemporal expression of thirteen candidate neurogenesis genes in the retina (Figures 4A, S2, and S3). In early retinal development (stage 21), the transcription factor *DpSoxB1* is homogeneously expressed across the retinal epithelium. At stage 23, the epithelium is divided across the apical-basal axis, with *DpSoxB1* segregated to the basal side of the retina and the receptor tyrosine kinase, *DpEphR*, segregated to the apical side. At stage 25 we see the first evidence of the terminal differentiation markers *DpRhodopsin* and *DpRetinochrome*, a cephalopod photopigment and photo-isomerase. At stage 27, the first evidence of the basal membrane is apparent, which is correlated with a loss of strict segregation of *DpSoxB1* and *DpEphR* expression. We find that *DpSoxB1* expression is never found posterior to the basal membrane; however, *DpEphR* is found on both sides of the membrane until hatching (stage 29). At stage 29, *DpEphR* is isolated to a subset of cells posterior to the basal membrane. Terminal differentiation markers span both sides of the basal membrane at stage 29. We hypothesize that *DpRhodopsin* is expressed exclusively in the photoreceptor cells, that the mRNA is being trafficked to the outer segment, and that *DpRetinochrome* is expressed in both the photoreceptor cells and support cells.

As found in other cephalopods, we report a lack of expression of the canonical neurogenic ELAV in the retina, *DpELAV*, an RNA-binding protein commonly found in differentiating neurons across species.[44–51] However, we do find that both cephalopod-specific *DpELAVL* paralogs are expressed in the developing retina and brain (Figure S3). bHLH factors *DpNeuroD* and *DpNeuroG*, both with orthologs that have roles in neural specification and differentiation in many animals, are expressed in the lateral lips and brain in *D. pealeii* and other cephalopods but are completely absent from the retina (Figure S3).[52–54]

This gene expression survey suggests differentiation trajectories in the retina (Figures 4B and 4C). *DpSoxB1* is a marker for retinal progenitor cells that are undergoing interkinetic nuclear migration in the pseudostratified epithelium. Homologs of SoxB1 are required to maintain neural precursor cells in vertebrates (Sox1, 2, and 3) and neuroblasts in *Drosophila* (SoxNeuro and Dichaete).[55–58] Cells differentiating into photoreceptor cells transition to *DpEphR*-positive cells and become post-mitotic. We hypothesize that *DpSoxB1* is intracellularly segregated to the cell bodies within the epithelium, while *DpEphR*-positive cells are the first cells to delaminate from the epithelium. Eventually, *DpEphR* expressing cells begin to express terminal differentiation markers and migrate from the apical side of the epithelium to behind the basal membrane. This leads to the dissolution of early retinal gene expression segregation and the emergence of terminally differentiated *DpRhodopsin*- and *DpRetinochrome*-expressing photoreceptor cells. Cells differentiating into support cells also start as *DpSoxB1*-positive retinal progenitor cells. This self-renewing population is maintained throughout development. As photoreceptor cells migrate behind the basal membrane, *DpSoxB1*-positive support cells begin to express *DpRetinochrome* and are found anterior in the retina, remaining in the cell cycle.[23] The *DpSoxB1*/*DpRetinochrome*-positive support cells may be a stem cell population contributing to ongoing growth.

Notch regulates retinal progenitor identity in the cephalopod

Our data show that *DpSoxB1* and *DpEphR* expression are similarly spatially segregated in the epithelium to cells in S phase and post-mitotic cells, respectively (Figures 2B and 5A–5C). Our BrdU chase experiments suggest that *DpSoxB1* cells likely become *DpEphR* cells over time. Notch signaling is a well-known regulator of cell-cycle exit and differentiation. Previous work showed that the loss of Notch signaling leads squid retinal cells to exit the cell cycle.[23] We were interested in understanding the role of Notch signaling in regulating cell fate trajectories. We first performed *in situ* hybridization for Notch signaling pathway members (Figures 5D and S4A). We find that *DpNotch* and *DpHes-1* expression is regionally correlated with *DpSoxB1* expression and progenitor identity (Figures 5D and S4A). We also find *DpNotch* expressed in mitotic, PH3-positive nuclei on the apical side of the retina (Figure 5E). Thus, inheritance of Notch mRNA may be an important part of maintaining progenitor cell identity.

To assess the role of Notch in cell fate we bathed embryos in the gamma-secretase inhibitor, N-[N-(3,5-difluorophenacetyl)-L-alanyl]-S-phenylglycine t-butyl ester (DAPT). DAPT impacts Notch signaling by inhibiting gamma-secretase from cleaving the Notch intracellular domain and entering the nucleus. DAPT has been shown to impact Notch signaling in the squid.[23] Embryos were treated with DAPT or DMSO, starting at stage 23 for 24 h. Eyes were dissected and pooled. RNA was extracted from three experimental and control samples and sequenced. We found 2,242 genes differentially expressed between DAPT and control eyes with a p value of less than 0.05 (Figures 5F–5H and S4B–S4F; Table S1). Comparing DAPT-treated to control eye samples showed both up- and down- regulation of neural and sensory markers, suggesting a shift in cell-type identity (Figure 5F). In addition, cell-cycle-related genes were downregulated, as expected (Figure 5G).[23] Finally, DAPT versus control eyes showed significant changes in cell signaling genes (Figure 5H).

To confirm changes in gene expression identified in the RNA-seq analysis, we performed *in situ* hybridization studies on control and DAPT-treated embryos (Figures 5I and S6). Specifically, we find a loss of *DpNotch* expression, a downregulation of *DpRhodopsin*, and a complete loss of *DpSoxB1* in DAPT-treated retinas (Figure 5I). We also observe a gain of expression of *DpEphR* and synaptic-transmission-related gene, *DpSec-1*, in the posterior retina, as well as ectopic expression of *DpVEGFR* in a subpopulation of cells in DAPT-treated retinas (Figure 5I). The complete loss of *DpSoxB1* and the ectopic expression of *DpEphR* shows that DAPT inhibition not only results in changes in cell-cycle state but also changes molecular fate in the squid retina. Unlike the consequence of Notch inhibition in the vertebrate retina, the cells do not appear to prematurely terminally differentiate but arrest at the *DpEphR* step in the trajectory.[59] These data suggest that Notch signaling is required to maintain retinal progenitor identity in addition to regulating cell-cycle exit in the squid.

DISCUSSION

We have characterized the epithelial organization and oscillatory nuclear behaviors of retinal progenitor cells in squid. We have defined molecular markers and the regionalization of progenitor,

Please cite this article in press as: Napoli et al., Cephalopod retinal development shows vertebrate-like mechanisms of neurogenesis, Current Biology (2022), https://doi.org/10.1016/j.cub.2022.10.027

CellPress

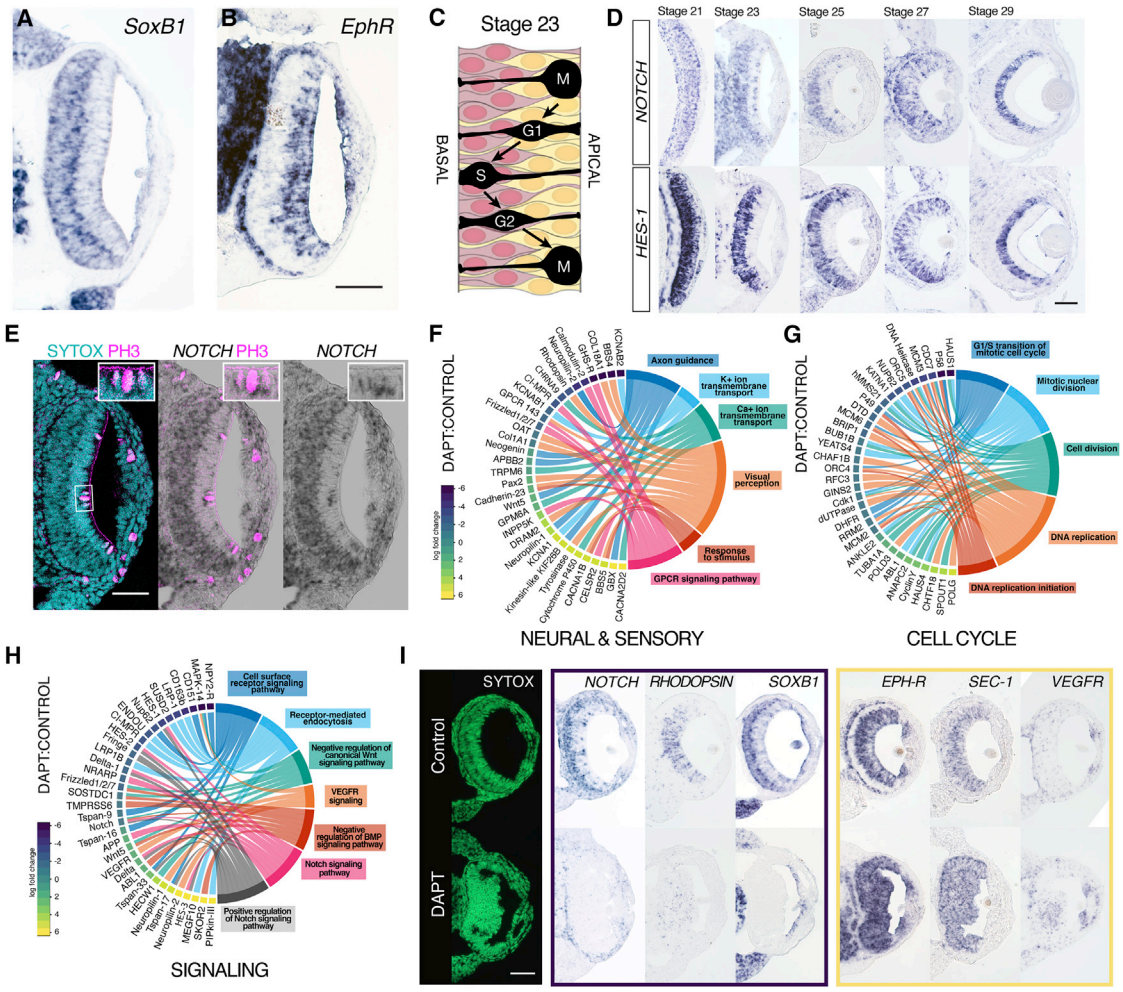

Figure 5. Notch signaling is required to maintain retinal progenitor cell identity

(A) *DpSoxB1* expression on the basal side of the retina at stage 23 in retinal progenitor cells.

(B) *DpEphR* expression on the apical side of the retina at stage 23 in post-mitotic cells. Scale bar, 50 μm.

(C) Schematic of nuclear migration within the pseudostratified retinal epithelium. Red (*DpSoxB1*) and yellow (*DpEphR*) color corresponds to gene expression and summary (Figures 3B and 3C).

(D) *DpNotch* and *DpHes-1* expression correlates with *DpSoxB1* expression in the retinal progenitor cell population. Scale bar, 50 μm.

(E) *DpNotch* expression on the apical side of the retinal epithelium correlates with PH3 expression. Scale bar, 50 μm.

(F–H) David GO-annotations of RNA-seq results of DAPT-inhibited eyes. Embryos treated with 20uM DAPT and DMSO control at stage 23 for 24 h. Eyes dissected for sequencing. All results shown have a p value < 0.05. Purple is downregulated genes, yellow is upregulated. (F) Neural and sensory genes. (G) Cell-cycle genes. (H) Signaling pathway genes. Color key is shared for all RNA-seq results. Names of genes are best BLAST hits in *Homo sapiens* or genes phylogenetically assessed here (Figure S2) or in previous work. *DpSoxB1* was found downregulated and *DpEphR* was found upregulated in the dataset, but these changes were not deemed statistically significant.

(I) *In situ* hybridization of control and DAPT-inhibited retinas. Embryos treated with 20 μM DAPT and DMSO control at stage 23 for 24 h and fixed immediately. Nuclear stain (SYTOX-green) shown in green in the first column. Selected downregulated genes in DAPT-treated embryos in the purple box on the left. Selected upregulated genes in DAPT-treated embryos in the yellow box on the right. *DpSoxB1* expression, the retinal progenitor marker, is lost from the retina in DAPT-treated embryos. *DpEphR* expression, the neuroblast marker, has expanded expression throughout the retina in DAPT-treated embryos. Scale bar, 50μm. See also Figures S2, S4, and S5 and Tables S1 and S2.

post-mitotic, and differentiated cells in the retina, and we have shown that Notch signaling regulates both cell-cycle and molecular identity during retinal development (Figures 4B, 4C, and 6A). These findings are the first detailed analysis of the developmental cell biology in the largest invertebrate nervous system. We can use this as a powerful, independent example of nervous system elaboration to enable a greater understanding of mechanisms that allow for the evolution of complex sensory organs.

The cell behaviors and organization we describe in the squid retina are unusual because of their unique similarity to early neurogenesis in vertebrate species (Figures 6A and 6B).[69,70] Pseudostratified epithelia and interkinetic nuclear migration have been observed in multiple tissue types and across multiple species and are thought to maximize mitoses during proliferative phases in development.[25,29,36,71–75] In the nervous system, pseudostratification was historically considered a vertebrate-specific

Please cite this article in press as: Napoli et al., Cephalopod retinal development shows vertebrate-like mechanisms of neurogenesis, Current Biology (2022), https://doi.org/10.1016/j.cub.2022.10.027

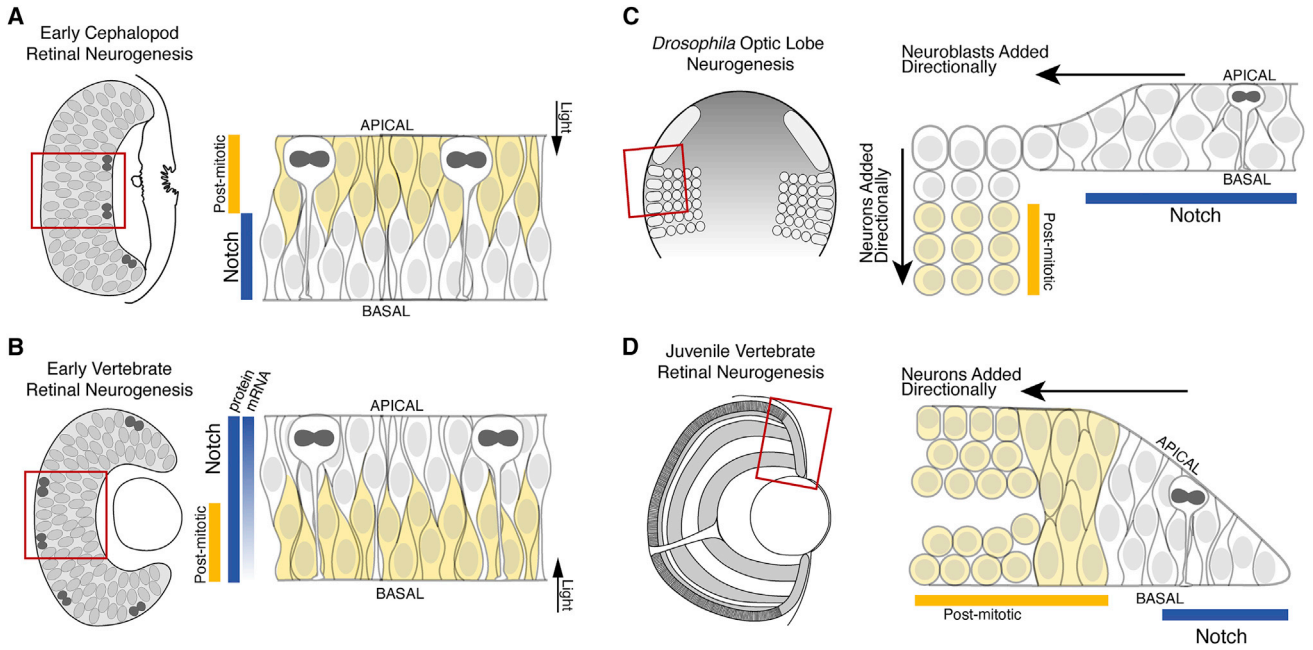

Figure 6. Summary of Notch signaling and early cell-cycle state in animal neurogenesis within pseudostratified epithelia

Organization of neurogenic epithelia shows similarity between the cephalopod retina and early vertebrate neurogenesis. Summarized Notch expression is mRNA unless otherwise noted. The yellow-colored cells show the organization of the first post-mitotic cells during development.

(A) Cartoon cross-section of the squid retina. Summary of retinal neurogenesis and *Notch* mRNA expression found in the current study. *DpNotch* mRNA is enriched basally (or posterior) and the first post-mitotic cells are found apically (or anterior).

(B) Cartoon cross-section of the developing vertebrate retina. *Notch* mRNA expression has been observed expressed in a gradient enriched on the apical side (or posterior).[60] Notch protein has been found uniformly expressed across the epithelium.[61] Retinal ganglion cells are the first cells to exit the cell cycle, differentiate, and migrate to the basal (anterior) side of the retina.[62]

(C and D) are examples of conveyor belt neurogenesis.[63] (C) Cartoon cross-section of the outer proliferative zone in the *Drosophila* optic lobe. The proliferative epithelium is *Notch*-positive.[64–66] Neuroblasts that have exited the epithelium continue to divide. (D) Cartoon cross-section of the juvenile zebrafish retina. Ciliary marginal zone contribution to juvenile and adult retinal neurogenesis and *Notch* expression is summarized.[63,67,68] The proliferative zone is segregated from the differentiated cells. See also Figure S2.

developmental trait, responsible for the large size of the central nervous system (Figure 6B).[25,72–75] Currently, the only other invertebrate neurogenic tissue where interkinetic nuclear migration has been well described is in the *Drosophila* optic lobe (Figure 6C).[54] In this case, the apicobasal distance of migration is significantly smaller than vertebrate neurogenic tissues and our observations in squid (Figure 6D).[29,76] Invertebrate neurogenesis, in the *Drosophila* optic lobe and elsewhere, is currently characterized by individual cells delaminating or ingressing from a neuroepithelium, sometimes dividing, and then migrating away from the progenitor population to organize and differentiate.[3,44,60,76–78] Neurogenesis in the *Drosophila* optic lobe has been compared with "conveyor belt" neurogenesis found in the zebrafish ciliary and tectal marginal zones, where, during long-term growth, cells are progressively added from the edge of a pseudostratified stem cell population (Figure 6D).[58] This is unlike embryonic vertebrate neurogenesis and the process described in the present study, where organization and differentiation within the neuroepithelium allows for tissue-level morphogenesis, such as neural tube closure or optic cup formation.[71]

In addition to maximizing proliferation, our data suggest an alternate function for pseudostratified epithelia. We show that Notch signaling is maintaining molecular identity of progenitor cells in the squid retina, and that the loss of Notch signaling leads to the expression of the post-mitotic marker *DpEphR*. Notably, we find the mRNA for genes associated with progenitor cell identity (*DpNotch, DpHes-1, DpSoxB1, and DpSoxB2*) localized basally within the epithelium. This asymmetrical localization is similar to mRNA gradients that have been reported during vertebrate neurogenesis.[79,80] Currently, the function of these mRNA gradients is not understood.[61] Our data reveal that *DpNotch* mRNA, localized basally, is found apically during mitosis, indicating that intracellular mRNA localization may enable the regulated segregation of RNA during symmetrical and asymmetrical cell divisions in densely packed epithelia (Figure 5E).

Although we have now confirmed that pseudostratified neurogenesis occurs in the retina, little is known about neurogenesis in the cephalopod brain. It has been reported that cells migrate from the lateral lip, an embryonic neurogenic tissue, to regions within the brain.[49] Pseudostratification of the lateral lips is not apparent, indicating that this development may resemble canonical invertebrate neurogenesis.[49,81] However, with a significantly larger brain than other spiralians, requiring long-distance cell migration, it is likely that cephalopods have evolved lineage-specific mechanisms to manage this process.

The evidence we have generated demonstrates that vertebrate-like cell behaviors during neurogenesis are not exclusive to the chordate lineage and identifies shared developmental

tools deployed to build large nervous systems. This is a novel example of developmental process homology, or the use of an ancestral developmental mechanism that may be independent of character identity.[82] This sheds light on cell behaviors and transcriptional modifications that may contribute to changes in allometry and cell-type variation found across the diversity of animal nervous systems. Ultimately, this work illuminates the necessity for phylogenetic sampling of cell-resolution expression and live-imaging data to better understand fundamental mechanisms in developmental biology.

STAR★METHODS

Detailed methods are provided in the online version of this paper and include the following:

- KEY RESOURCES TABLE
- RESOURCE AVAILABILITY
  - Lead contact
  - Materials availability
  - Data and code availability
- EXPERIMENTAL MODEL AND SUBJECT DETAILS
- METHOD DETAILS
  - *Cloning and* in situ *Hybridization*
  - Ex ovo *and Drug Treatments*
- QUANTIFICATION AND STATISTICAL ANALYSIS
  - Phylogenetic Analysis
  - Imaging analysis
  - RNA-seq and Bioinformatics

SUPPLEMENTAL INFORMATION

Supplemental information can be found online at https://doi.org/10.1016/j.cub.2022.10.027.

ACKNOWLEDGMENTS

This work was supported by funding from the NIH Director 1DP5OD023111-01 to K.M.K. and the John Harvard Distinguished Science Fellowship to K.M.K. We would like to thank the Srivastava lab for helpful discussions and Mansi Srivastava, Andrew Murray, Nicholas Bellono, Lauren O'Connell, and Jeffrey Gross for comments on the manuscript. We thank Kevin Woods and the John Harvard Distinguished Science Fellows community for support. We thank the Marine Biological Labs and the Marine Resources Center for assistance and access to embryos.

AUTHOR CONTRIBUTIONS

K.M.K. conceptualized the project. K.M.K., F.R.N., C.M.D., and S.N. designed the experiments. K.M.K., F.R.N., C.M.D., S.N., A.R.Z., and A.L. performed experiments. K.J.M. and K.M.K. performed phylogenetic and statistical analyses. K.M.K., C.M.D., and K.J.M. wrote the manuscript, with editing and review from F.R.N., S.N., A.R.Z., and A.L. K.M.K. acquired the funding.

DECLARATION OF INTERESTS

The authors declare no competing interests.

Received: June 20, 2022
Revised: September 30, 2022
Accepted: October 14, 2022
Published: November 9, 2022

REFERENCES

1. Gagnon, Y.L., Sutton, T.T., and Johnsen, S. (2013). Visual acuity in pelagic fishes and mollusks. Vision Res. *92*, 1–9. https://doi.org/10.1016/j.visres.2013.08.007.
2. Packard, A. (1972). Cephalopods and fish: the limits of convergence. Biol. Rev. *47*, 241–307. https://doi.org/10.1111/j.1469-185X.1972.tb00975.x.
3. Hartenstein, V., and Stollewerk, A. (2015). The evolution of early neurogenesis. Dev. Cell *32*, 390–407. https://doi.org/10.1016/j.devcel.2015.02.004.
4. Bertrand, V., and Hobert, O. (2010). Lineage programming: navigating through transient regulatory states via binary decisions. Curr. Opin. Genet. Dev. *20*, 362–368. https://doi.org/10.1016/j.gde.2010.04.010.
5. Zechner, C., Nerli, E., and Norden, C. (2020). Stochasticity and determinism in cell fate decisions. Development *147*, dev181495. https://doi.org/10.1242/dev.181495.
6. Young, J.Z. (1962). The retina of cephalopods and its degeneration after optic nerve section. Philos. Trans. R. Soc. Lond. B *245*, 1–18.
7. Simpson, J.H. (2009). Mapping and manipulating neural circuits in the fly brain. Adv. Genet. *65*, 79–143.
8. Azevedo, F.A., Carvalho, L.R., Grinberg, L.T., Farfel, J.M., Ferretti, R.E., Leite, R.E., Jacob Filho, W.J., Lent, R., and Herculano-Houzel, S. (2009). Equal numbers of neuronal and nonneuronal cells make the human brain an isometrically scaled-up primate brain. J. Comp. Neurol. *513*, 532–541.
9. Herculano-Houzel, S., Mota, B., and Lent, R. (2006). Cellular scaling rules for rodent brains. Proc. Natl. Acad. Sci. USA *103*, 12138–12143.
10. Young, J.Z. (1963, March). The number and sizes of nerve cells in Octopus. Proc. Zool. Soc. Lond. *140*, 229–254.
11. Hinsch, K., and Zupanc, G.K.H. (2007). Generation and long-term persistence of new neurons in the adult zebrafish brain: a quantitative analysis. Neuroscience *146*, 679–696.
12. Skogh, C., Garm, A., Nilsson, D.E., and Ekström, P. (2006). Bilaterally symmetrical rhopalial nervous system of the box jellyfish Tripedalia Cystophora. J. Morphol. *267*, 1391–1405.
13. Garm, A., Poussart, Y., Parkefelt, L., Ekström, P., and Nilsson, D.E. (2007). The ring nerve of the box jellyfish Tripedalia Cystophora. Cell Tissue Res. *329*, 147–157.
14. Cash, D., and Carew, T.J. (1989). A quantitative analysis of the development of the central nervous system in juvenile Aplysia californica. J. Neurobiol. *20*, 25–47.
15. Hardie, R.C. (1985). Functional organization of the fly retina. Progress in Sensory Physiology (Springer), pp. 1–79.
16. Curcio, C.A., Sloan, K.R., Kalina, R.E., and Hendrickson, A.E. (1990). Human photoreceptor topography. J. Comp. Neurol. *292*, 497–523.
17. Jeon, C.J., Strettoi, E., and Masland, R.H. (1998). The major cell populations of the mouse retina. J. Neurosci. *18*, 8936–8946.
18. Jacklet, J.W., Alvarez, R., and Bernstein, B. (1972). Ultrastructure of the eye of Aplysia. J. Ultrastruct. Res. *38*, 246–261.
19. Arnold, J.M. (1965). Normal embryonic stages of the squid, loligo PEALII (Lesueur). Biol. Bull. *128*, 24–32. https://doi.org/10.2307/1539386.
20. Yamamoto, T., Tasaki, K., Sugawara, Y., and Tonosaki, A. (1965). Fine structure of the octopus retina. J. Cell Biol. *25*, 345–359. https://doi.org/10.1083/jcb.25.2.345.
21. Young, J.Z. (1974). The central nervous system of Loligo. I. The optic lobe. Philos. Trans. R. Soc. Lond. B Biol. Sci. *267*, 263–302. https://doi.org/10.1098/rstb.1974.0002.
22. Gavriouchkina, D., Tan, Y., Künzli-Ziadi, F., Hasegawa, Y., Piovani, L., Zhang, L., Sugimoto, C., Luscombe, N., Marlétaz, F., and Rokhsar, D.S. (2022). A single-cell atlas of bobtail squid visual and nervous system highlights molecular principles of convergent evolution. Preprint at bioRxiv. https://doi.org/10.1101/2022.05.26.490366.

23. Koenig, K.M., Sun, P., Meyer, E., and Gross, J.M. (2016). Eye development and photoreceptor differentiation in the cephalopod Doryteuthis pealeii. Development *143*, 3168–3181. https://doi.org/10.1242/dev.134254.

24. Koenig, K.M., and Gross, J.M. (2020). Evolution and development of complex eyes: a celebration of diversity. Development *147*, dev182923. https://doi.org/10.1242/dev.182923.

25. Kosodo, Y. (2012). Interkinetic nuclear migration: beyond a hallmark of neurogenesis. Cell. Mol. Life Sci. *69*, 2727–2738. https://doi.org/10.1007/s00018-012-0952-2.

26. Taverna, E., Götz, M., and Huttner, W.B. (2014). The cell biology of neurogenesis: toward an understanding of the development and evolution of the neocortex. Annu. Rev. Cell Dev. Biol. *30*, 465–502. https://doi.org/10.1146/annurev-cellbio-101011-155801.

27. Norden, C. (2017). Pseudostratified epithelia – cell biology, diversity and roles in organ formation at a glance. J. Cell Sci. *130*, 1859–1863. https://doi.org/10.1242/jcs.192997.

28. Baye, L.M., and Link, B.A. (2008). Nuclear migration during retinal development. Brain Res. *1192*, 29–36. https://doi.org/10.1016/j.brainres.2007.05.021.

29. Strzyz, P.J., Matejcic, M., and Norden, C. (2016). Heterogeneity, cell biology and tissue mechanics of pseudostratified epithelia: coordination of cell divisions and growth in tightly packed tissues. Int. Rev. Cell Mol. Biol. *325*, 89–118. https://doi.org/10.1016/bs.ircmb.2016.02.004.

30. Dash, S., Dang, C.A., Beebe, D.C., and Lachke, S.A. (2015). Deficiency of the RNA binding protein caprin2 causes lens defects and features of peters anomaly. Dev. Dyn. *244*, 1313–1327.

31. Yanakieva, I., Erzberger, A., Matejčić, M., Modes, C.D., and Norden, C. (2019). Cell and tissue morphology determine actin-dependent nuclear migration mechanisms in neuroepithelia. J. Cell Biol. *218*, 3272–3289.

32. Norden, C., Young, S., Link, B.A., and Harris, W.A. (2009). Actomyosin is the main driver of interkinetic nuclear migration in the retina. Cell *138*, 1195–1208. https://doi.org/10.1016/j.cell.2009.06.032.

33. Nickerson, P.E., Ronellenfitch, K.M., Csuzdi, N.F., Boyd, J.D., Howard, P.L., Delaney, K.R., and Chow, R.L. (2013). Live imaging and analysis of postnatal mouse retinal development. BMC Dev. Biol. *13*, 24.

34. Barrasso, A.P., Wang, S., Tong, X., Christiansen, A.E., Larina, I.V., and Poché, R.A. (2018). Live imaging of developing mouse retinal slices. Neural Dev. *13*, 23.

35. Schindelin, J., Arganda-Carreras, I., Frise, E., Kaynig, V., Longair, M., Pietzsch, T., Preibisch, S., Rueden, C., Saalfeld, S., Schmid, B., et al. (2012). Fiji: an open-source platform for biological-image analysis. Nat. Methods *9*, 676–682. https://doi.org/10.1038/nmeth.2019.

36. Meyer, E.J., Ikmi, A., and Gibson, M.C. (2011). Interkinetic nuclear migration is a broadly conserved feature of cell division in pseudostratified epithelia. Curr. Biol. *21*, 485–491. https://doi.org/10.1016/j.cub.2011.02.002.

37. Tsai, J.W., Lian, W.N., Kemal, S., Kriegstein, A.R., and Vallee, R.B. (2010). Kinesin 3 and cytoplasmic dynein mediate interkinetic nuclear migration in neural stem cells. Nat. Neurosci. *13*, 1463–1471. https://doi.org/10.1038/nn.2665.

38. Pearce, T.L., and Zwaan, J. (1970). A light and electron microscopic study of cell behavior and microtubules in the embryonic chicken lens using Colcemid. J. Embryol. Exp. Morphol. *23*, 491–507. https://doi.org/10.1242/dev.23.2.491.

39. Knoblich, J.A. (2008). Mechanisms of asymmetric stem cell division. Cell *132*, 583–597. https://doi.org/10.1016/j.cell.2008.02.007.

40. Morin, X., and Bellaïche, Y. (2011). Mitotic spindle orientation in asymmetric and symmetric cell divisions during animal development. Dev. Cell *21*, 102–119. https://doi.org/10.1016/j.devcel.2011.06.012.

41. Dehay, C., and Kennedy, H. (2007). Cell-cycle control and cortical development. Nat. Rev. Neurosci. *8*, 438–450. https://doi.org/10.1038/nrn2097.

42. Yu, F., Kuo, C.T., and Jan, Y.N. (2006). Drosophila neuroblast asymmetric cell division: recent advances and implications for stem cell biology. Neuron *51*, 13–20. https://doi.org/10.1016/j.neuron.2006.06.016.

43. Zigman, M., Cayouette, M., Charalambous, C., Schleiffer, A., Hoeller, O., Dunican, D., McCudden, C.R., Firnberg, N., Barres, B.A., Siderovski, D.P., and Knoblich, J.A. (2005). Mammalian inscuteable regulates spindle orientation and cell fate in the developing retina. Neuron *48*, 539–545. https://doi.org/10.1016/j.neuron.2005.09.030.

44. Meyer, N.P., and Seaver, E.C. (2009). Neurogenesis in an annelid: characterization of brain neural precursors in the polychaete Capitella sp. I. Dev. Biol. *335*, 237–252. https://doi.org/10.1016/j.ydbio.2009.06.017.

45. Akamatsu, W., Fujihara, H., Mitsuhashi, T., Yano, M., Shibata, S., Hayakawa, Y., Okano, H.J., Sakakibara, S.-I., Takano, H., Takano, T., et al. (2005). The RNA-binding protein HuD regulates neuronal cell identity and maturation. Proc. Natl. Acad. Sci. USA *102*, 4625–4630. https://doi.org/10.1073/pnas.0407523102.

46. Denes, A.S., Jékely, G., Steinmetz, P.R.H., Raible, F., Snyman, H., Prud'homme, B., Ferrier, D.E., Balavoine, G., and Arendt, D. (2007). Molecular architecture of annelid nerve cord supports common origin of nervous system centralization in bilateria. Cell *129*, 277–288. https://doi.org/10.1016/j.cell.2007.02.040.

47. Nakanishi, N., Renfer, E., Technau, U., and Rentzsch, F. (2012). Nervous systems of the sea anemone Nematostella vectensis are generated by ectoderm and endoderm and shaped by distinct mechanisms. Development *139*, 347–357. https://doi.org/10.1242/dev.071902.

48. Nomaksteinsky, M., Röttinger, E., Dufour, H.D., Chettouh, Z., Lowe, C.J., Martindale, M.Q., and Brunet, J.F. (2009). Centralization of the deuterostome nervous system predates chordates. Curr. Biol. *19*, 1264–1269. https://doi.org/10.1016/j.cub.2009.05.063.

49. Deryckere, A., Styfhals, R., Elagoz, A.M., Maes, G.E., and Seuntjens, E. (2021). Identification of neural progenitor cells and their progeny reveals long distance migration in the developing octopus brain. eLife *10*, e69161. https://doi.org/10.7554/eLife.69161.

50. Buresi, A., Canali, E., Bonnaud, L., and Baratte, S. (2013). Delayed and asynchronous ganglionic maturation during cephalopod neurogenesis as evidenced by Sof-elav1 expression in embryos of Sepia officinalis (Mollusca, Cephalopoda). J. Comp. Neurol. *521*, 1482–1496. https://doi.org/10.1002/cne.23231.

51. Shigeno, S., Parnaik, R., Albertin, C.B., and Ragsdale, C.W. (2015). Evidence for a cordal, not ganglionic, pattern of cephalopod brain neurogenesis. Zoological Lett. *1*, 26. https://doi.org/10.1186/s40851-015-0026-z.

52. Buescher, M., Hing, F.S., and Chia, W. (2002). Formation of neuroblasts in the embryonic central nervous system of Drosophila melanogaster is controlled by SoxNeuro. Development *129*, 4193–4203. https://www.ncbi.nlm.nih.gov/pubmed/12183372.

53. Bylund, M., Andersson, E., Novitch, B.G., and Muhr, J. (2003). Vertebrate neurogenesis is counteracted by Sox1–3 activity. Nat. Neurosci. *6*, 1162–1168. https://doi.org/10.1038/nn1131.

54. Ferrero, E., Fischer, B., and Russell, S. (2014). SoxNeuro orchestrates central nervous system specification and differentiation in Drosophila and is only partially redundant with Dichaete. Genome Biol. *15*, R74. https://doi.org/10.1186/gb-2014-15-5-r74.

55. Holmberg, J., Hansson, E., Malewicz, M., Sandberg, M., Perlmann, T., Lendahl, U., and Muhr, J. (2008). SoxB1 transcription factors and Notch signaling use distinct mechanisms to regulate proneural gene function and neural progenitor differentiation. Development *135*, 1843–1851. https://doi.org/10.1242/dev.020180.

56. Neriec, N., and Desplan, C. (2014). Different ways to make neurons: parallel evolution in the SoxB family. Genome Biol. *15*, 116. https://doi.org/10.1186/gb4177.

57. Overton, P.M., Meadows, L.A., Urban, J., and Russell, S. (2002). Evidence for differential and redundant function of the Sox genes Dichaete and SoxN during CNS development in Drosophila.

Development *129*, 4219–4228. https://www.ncbi.nlm.nih.gov/pubmed/12183374.

58. Taranova, O.V., Magness, S.T., Fagan, B.M., Wu, Y., Surzenko, N., Hutton, S.R., and Pevny, L.H. (2006). SOX2 is a dose-dependent regulator of retinal neural progenitor competence. Genes Dev. *20*, 1187–1202. https://doi.org/10.1101/gad.1407906.
59. Perron, M., and Harris, W.A. (2000). Determination of vertebrate retinal progenitor cell fate by the Notch pathway and basic helix-loop-helix transcription factors. Cell. Mol. Life Sci. *57*, 215–223. https://doi.org/10.1007/PL00000685.
60. Byrne, J.H. (2019). The Oxford Handbook of Invertebrate Neurobiology (Oxford University Press). https://play.google.com/store/books/details?id=O_iEDwAAQBAJ.
61. Nerli, E., Rocha-Martins, M., and Norden, C. (2020). Asymmetric neurogenic commitment of retinal progenitors involves Notch through the endocytic pathway. eLife *9*, e60462. https://doi.org/10.7554/eLife.60462.
62. Seritrakul, P., and Gross, J.M. (2017). Tet-mediated DNA hydroxymethylation regulates retinal neurogenesis by modulating cell-extrinsic signaling pathways. PLoS Genet. *13*, e1006987. https://doi.org/10.1371/journal.pgen.1006987.
63. Joly, J.S., Recher, G., Brombin, A., Ngo, K., and Hartenstein, V. (2016). A conserved developmental mechanism builds complex visual systems in insects and vertebrates. Curr. Biol. *26*, R1001–R1009. https://doi.org/10.1016/j.cub.2016.08.017.
64. Chen, Y.C., and Desplan, C. (2020). Gene regulatory networks during the development of the Drosophila visual system. Curr. Top. Dev. Biol. *139*, 89–125. https://doi.org/10.1016/bs.ctdb.2020.02.010.
65. Egger, B., Gold, K.S., and Brand, A.H. (2010). Notch regulates the switch from symmetric to asymmetric neural stem cell division in the Drosophila optic lobe. Development *137*, 2981–2987. https://doi.org/10.1242/dev.051250.
66. Wang, W., Liu, W., Wang, Y., Zhou, L., Tang, X., and Luo, H. (2011). Notch signaling regulates neuroepithelial stem cell maintenance and neuroblast formation in Drosophila optic lobe development. Dev. Biol. *350*, 414–428. https://doi.org/10.1016/j.ydbio.2010.12.002.
67. Harris, W.A., and Perron, M. (1998). Molecular recapitulation: the growth of the vertebrate retina. Int. J. Dev. Biol. *42*, 299–304 https://www.ncbi.nlm.nih.gov/pubmed/9654012.
68. Raymond, P.A., Barthel, L.K., Bernardos, R.L., and Perkowski, J.J. (2006). Molecular characterization of retinal stem cells and their niches in adult zebrafish. BMC Dev. Biol. *6*, 36. https://doi.org/10.1186/1471-213X-6-36.
69. Agathocleous, M., and Harris, W.A. (2009). From progenitors to differentiated cells in the vertebrate retina. Annu. Rev. Cell Dev. Biol. *25*, 45–69. https://doi.org/10.1146/annurev.cellbio.042308.113259.
70. Livesey, F.J., and Cepko, C.L. (2001). Vertebrate neural cell-fate determination: lessons from the retina. Nat. Rev. Neurosci. *2*, 109–118. https://doi.org/10.1038/35053522.
71. Spear, P.C., and Erickson, C.A. (2012). Interkinetic nuclear migration: a mysterious process in search of a function. Develop. Growth Differ. *54*, 306–316. https://doi.org/10.1111/j.1440-169X.2012.01342.x.
72. Smart, I.H. (1972). Proliferative characteristics of the ependymal layer during the early development of the mouse diencephalon, as revealed by recording the number, location, and plane of cleavage of mitotic figures. J. Anat. *113*, 109–129.
73. Smart, I.H. (1972). Proliferative characteristics of the ependymal layer during the early development of the spinal cord in the mouse. J. Anat. *111*, 365–380.
74. Fish, J.L., Dehay, C., Kennedy, H., and Huttner, W.B. (2008). Making bigger brains–the evolution of neural-progenitor-cell division. J. Cell Sci. *121*, 2783–2793.
75. Taverna, E., and Huttner, W.B. (2010). Neural progenitor nuclei IN motion. Neuron *67*, 906–914.
76. Egger, B., Boone, J.Q., Stevens, N.R., Brand, A.H., and Doe, C.Q. (2007). Regulation of spindle orientation and neural stem cell fate in the Drosophila optic lobe. Neural Dev. *2*, 1. https://doi.org/10.1186/1749-8104-2-1.
77. Holguera, I., and Desplan, C. (2018). Neuronal specification in space and time. Science *362*, 176–180. https://doi.org/10.1126/science.aas9435.
78. Sur, A., Renfro, A., Bergmann, P.J., and Meyer, N.P. (2020). Investigating cellular and molecular mechanisms of neurogenesis in Capitella teleta sheds light on the ancestor of Annelida. BMC Evol. Biol. *20*, 84. https://doi.org/10.1186/s12862-020-01636-1.
79. Del Bene, F., Wehman, A.M., Link, B.A., and Baier, H. (2008). Regulation of neurogenesis by interkinetic nuclear migration through an apical-basal notch gradient. Cell *134*, 1055–1065. https://doi.org/10.1016/j.cell.2008.07.017.
80. Murciano, A., Zamora, J., López-Sánchez, J., and Frade, J.M. (2002). Interkinetic nuclear movement may provide spatial clues to the regulation of neurogenesis. Mol. Cell. Neurosci. *21*, 285–300.
81. Marthy, H.-J. (1987). Ontogenesis of the nervous system in cephalopods. Nervous Systems in Invertebrates (Springer), pp. 443–459. https://doi.org/10.1007/978-1-4613-1955-9_15.
82. DiFrisco, J., and Jaeger, J. (2021). Homology of process: developmental dynamics in comparative biology. Interface Focus *11*, 20210007.
83. Ershov, D., Phan, M.S., Pylvänäinen, J.W., Rigaud, S.U., Le Blanc, L., Charles-Orszag, A., Conway, J.R., Laine, R.F., Roy, N.H., Bonazzi, D., et al. (2021). Bringing TrackMate in the era of machine-learning and deep-learning. Preprint at bioRxiv. https://doi.org/10.1101/2021.09.03.458852.
84. Wu, Z., Wang, X., and Zhang, X. (2011). Using non-uniform read distribution models to improve isoform expression inference in RNA-Seq. Bioinformatics *27*, 502–508.
85. Langmead, B., and Salzberg, S.L. (2012). Fast gapped-read alignment with Bowtie 2. Nat. Methods *9*, 357–359. https://doi.org/10.1038/nmeth.1923.
86. Bray, N.L., Pimentel, H., Melsted, P., and Pachter, L. (2016). Near-optimal probabilistic RNA-seq quantification. Nat. Biotechnol. *34*, 525–527. https://doi.org/10.1038/nbt.3519.
87. Love, M.I., Huber, W., and Anders, S. (2014). Moderated estimation of fold change and dispersion for RNA-seq data with DESeq2. Genome Biol. *15*, 550. https://doi.org/10.1186/s13059-014-0550-8.
88. Huang, D.W., Sherman, B.T., Tan, Q., Kir, J., Liu, D., Bryant, D., Guo, Y., Stephens, R., Baseler, M.W., Lane, H.C., and Lempicki, R.A. (2007). DAVID Bioinformatics Resources: expanded annotation database and novel algorithms to better extract biology from large gene lists. Nucleic Acids Res. *35*, W169–W175. https://doi.org/10.1093/nar/gkm415.
89. Walter, W., Sánchez-Cabo, F., and Ricote, M. (2015). GOplot: An R package for visually combining expression data with functional analysis. Bioinformatics *31*, 2912–2914. https://doi.org/10.1093/bioinformatics/btv300.
90. Warnes, G.R., Bolker, B., Bonebakker, L., Gentleman, R., Humber, W., Liaw, A., Lumley, T., Maechler, M., Magnusson, A., Moeller, S., et al. (2015). Gplots: various R programming tools for plotting data. R, version 2.17.0. http://CRAN.R-project.org/package=gplots.
91. Goedhart, J., and Luijsterburg, M.S. (2020). VolcaNoseR is a web app for creating, exploring, labeling and sharing volcano plots. Sci. Rep. *10*, 20560. https://doi.org/10.1038/s41598-020-76603-3.
92. Altschul, S.F., Gish, W., Miller, W., Myers, E.W., and Lipman, D.J. (1990). Basic local alignment search tool. J. Mol. Biol. *215*, 403–410. https://doi.org/10.1016/S0022-2836(05)80360-2.
93. Katoh, K., and Standley, D.M. (2013). MAFFT multiple sequence alignment software version 7: improvements in performance and usability. Mol. Biol. Evol. *30*, 772–780. https://doi.org/10.1093/molbev/mst010.
94. Price, M.N., Dehal, P.S., and Arkin, A.P. (2010). FastTree 2--approximately maximum-likelihood trees for large alignments. PLoS One *5*, e9490. https://doi.org/10.1371/journal.pone.0009490.

95. Minh, B.Q., Schmidt, H.A., Chernomor, O., Schrempf, D., Woodhams, M.D., von Haeseler, A., and Lanfear, R. (2020). Corrigendum to: IQ-TREE 2: New models and efficient methods for phylogenetic inference in the genomic era. Mol. Biol. Evol. *37*, 2461. https://doi.org/10.1093/molbev/msaa131.

96. Neal, S., McCulloch, K.J., Napoli, F., Daly, C.M., Coleman, J.H., and Koenig, K.M. (2022). Co-option of the limb patterning program in cephalopod lens development. BMC biol. *20*, 1. https://doi.org/10.1101/2021.04.22.441006.

97. Hwang, H.H., Wang, C.H., Chen, H.H., Ho, J.F., Chi, S.F., Huang, F.C., and Yen, H.E. (2019). Effective Agrobacterium-mediated transformation protocols for callus and roots of halophyte ice plant (Mesembryanthemum crystallinum). Bot. Stud. *60*, 1.

98. Chien, S., Simchon, S., Abbott, R.E., and Jan, K.M. (1977). Surface adsorption of dextrans on human red cell membrane. J. Colloid Interface Sci. *62*, 461–470.

99. Schnitzler, C.E., Simmons, D.K., Pang, K., Martindale, M.Q., and Baxevanis, A.D. (2014). Expression of multiple Sox genes through embryonic development in the ctenophore Mnemiopsis leidyi is spatially restricted to zones of cell proliferation. EvoDevo *5*, 15. https://doi.org/10.1186/2041-9139-5-15.

100. Soneson, C., Love, M.I., and Robinson, M.D. (2015). Differential analyses for RNA-seq: transcript-level estimates improve gene-level inferences. F1000Res *4*, 1521. https://doi.org/10.12688/f1000research.7563.2.

Please cite this article in press as: Napoli et al., Cephalopod retinal development shows vertebrate-like mechanisms of neurogenesis, Current Biology (2022), https://doi.org/10.1016/j.cub.2022.10.027

STAR★METHODS

KEY RESOURCES TABLE

REAGENT or RESOURCE	SOURCE	IDENTIFIER
Antibodies		
BrdU antibody	Abcam	Cat# Ab6326; RRID: AB_305426
Phosphohistone H3	Sigma Aldrich	Cat# 06-570
Goat anti rat Alexa Fluor 488	Invitrogen	Cat# A-11006; RRID: AB_2534074
Goat anti rabbit Alexa Fluor 647	Invitrogen	Cat# A-31573; RRID: AB_2536183
Chemicals, peptides, and recombinant proteins		
Nocodazole	Sigma Aldrich	Cat# M1404-2MG
Cytochalasin D	Sigma-Aldrich	Cat# C8273-1MG
TRIzol	Invitrogen	Cat# 15596026
Dextran Alexa Fluor 488 10,000 MW	Invitrogen	Cat# D22910
Sytox Green	Invitrogen	Cat# S7020
Mounting Medium for IHC	Abcam	Cat# ab64230
Critical commercial assays		
gDNA eliminator mini-spin column	Qiagen	Cat# 1030958
Kapa mRNA-Hyper Prep kit with Poly-A selection	Roche	Cat# 08098115702
pGEM-T Easy vector	Promega	Cat# A1360
Deposited data		
DAPT:Control RNA-seq raw data	This paper	GenBank: PRJNA794156
D. pealeii mRNA sequences	This paper	OM481467-OM481487
Multiple sequence alignments and phylogenetic trees	This paper	Dryad Data: https://doi.org/10.5061/dryad.rr4xgxdc4
Assembled and annotated embryonic transcriptome for mapping	Koenig et al.[23]	https://orcid.org/0000-0001-6093-2262
Experimental models: Organisms/strains		
Doryteuthis pealeii	Marine Resources Center, Marine Biological Labs	N/A
Oligonucleotides		
Primers sequences, see Table S2	This paper	N/A
Software and algorithms		
FIJI 2.1.10	Schindelin et al.[35]	https://imagej.net/software/fiji/downloads
Coordinate Shift	Housei Wada	https://signaling.riken.jp/en/en-tools/imagej/
Trackmate 7.7.2	Ershov et al.[83]	https://imagej.net/plugins/trackmate/
TrimGalore! v3	Wu et al.[84]	https://www.bioinformatics.babraham.ac.uk/projects/trim_galore/
Bowtie2	Langmead et al.[85]	http://bowtie-bio.sourceforge.net/bowtie2/index.shtml
Kallisto	Bray et al.[86]	https://pachterlab.github.io/kallisto/
DESeq2	Love et al.[87]	https://bioconductor.org/packages/release/bioc/html/DESeq2.html
DAVID	Huang et al.[88]	https://david.ncifcrf.gov/
GOPlot	Walter et al.[89]	https://sourceforge.net/projects/gplot/
gplots	Warnes et al.[90]	https://cran.r-project.org/web/packages/gplots/index.html
VolcaNoseR	Goedhart et al.[91]	https://huygens.science.uva.nl/VolcaNoseR/

(*Continued on next page*)

Please cite this article in press as: Napoli et al., Cephalopod retinal development shows vertebrate-like mechanisms of neurogenesis, Current Biology (2022), https://doi.org/10.1016/j.cub.2022.10.027

Continued

REAGENT or RESOURCE	SOURCE	IDENTIFIER
BLAST	Altschul et al.[92]	https://blast.ncbi.nlm.nih.gov/Blast.cgi
MAFFT v.7.450	Katoh et al.[93]	https://mafft.cbrc.jp/alignment/software/
FastTree2 v.2.1.11	Price et al.[94]	http://www.microbesonline.org/fasttree/
IQ-TREE 2 v.2.1.0	Minh et al.[95]	http://www.iqtree.org/
Photoshop 2020	Adobe	https://www.adobe.com/products/photoshop.html
Geneious	Dotmatics	https://www.geneious.com/

RESOURCE AVAILABILITY

Lead contact

Further information and requests for resources and reagents should be directed to and will be fulfilled by the lead contact, Kristen Koenig (kmkoenig@fas.harvard.edu).

Materials availability

All unique/stable reagents generated in this study are available from the lead contact.

Data and code availability

RNA-seq data have been deposited at GenBank and Dryad Digital Repository are publicly available as of the date of publication. Accession numbers are listed in the key resources table. Any additional information required to reanalyze the data reported in this paper is available from the lead contact upon request. This study did not generate any unique code.

EXPERIMENTAL MODEL AND SUBJECT DETAILS

Doryteuthis pealeii egg sacks were obtained from the Marine Biological Labs. Egg sacks were kept at 20 degrees Celsius in 20 gallon aquaria in artificial seawater under a day/night cycle. Although not required, European guidelines for cephalopod research were followed.

METHOD DETAILS

Cloning and in situ *Hybridization*

Primers were designed using Primer3 in the Geneious software package version 2020.04 (https://www.geneious.com) and primer sequences are reported in Table S2. Genes were cloned into pGEM-T Easy vector and confirmed with Sanger sequencing and DIG-labeled RNA probes were synthesized as previously reported.[23] Embryos were fixed overnight at 4 degrees Celsius, washed and dehydrated stepwise into 100% ethanol. Embryos were embedded, paraffin sectioned and *in situ* hybridization was performed as previously reported.[96] All *in situs* were replicated in at least three embryos, across multiple separate *in situ* experiments. Slides were stained overnight with SYTOX-Green 1:1000 overnight, mounted using ImmunoHistoMount (Abcam) and imaged on a Zeiss Axioskop 2.

BrdU Experiments

Embryos were bathed in BrdU (10 mM) in pen-strep seawater for 10 minutes as previously described.[23] Embryos were fixed immediately and the remaining embryos were moved into pen-strep seawater. Groups of 10-15 embryos were fixed every ten minutes for two hours. Embryos were fixed overnight at 4 degrees and washed out into PBS-Tween. Embryos were stepped into 30% sucrose and embedded in tissue freezing medium and sectioned as previously described.[23] Antigen-retrieval and immunofluorescence were performed as previously described.[23] BrdU antibody (Abcam ab6326) at concentration 1:250. Phosphohistone H3 antibody (Sigma-Aldrich 06-570) was used at concentration 1:300. Secondary antibodies goat anti-rat Alexa Fluor 488 and goat anti rabbit Alexa Fluor 647 (Invitrogen). Sections were counterstained with SYTOX Green at 1:1000. Sections were imaged on a Zeiss LSM 880 or Zeiss LSM 980.

Live-imaging experiments

Embryos were dissected from egg cases. Previous studies have shown non-specific labeling of cell membranes or cell walls with exposure to fluorescently labeled Dextran.[97,98] This is also the case in squid. The vitreous space was injected using a pico-liter microinjector with Dextran Alexa Fluor 488 10,000 MW (D22910) at stage 23. Ubiquitous membrane labeling was apparent within a half hour of injection. Embryos were embedded in 1% low melt agarose in seawater and mounted in cover glass bottom dishes (100503-366). Embryos were immersed in pen strep seawater. Embryos were imaged on a Zeiss 880. Embryos were imaged every ten minutes for at least nine hours.

Please cite this article in press as: Napoli et al., Cephalopod retinal development shows vertebrate-like mechanisms of neurogenesis, Current Biology (2022), https://doi.org/10.1016/j.cub.2022.10.027

Ex ovo *and Drug Treatments*

Embryos were treated in 20uM DAPT solution or DMSO control in filter-sterilized, Pen-Strep seawater starting at stage 23 for 24 hours and fixed immediately as previously described.[23] Embryos were bathed in 5uM Nocodazole (M1404-2MG, Sigma-Aldrich) and 5uM Cytochalasin D (C8273-1MG, Sigma-Aldrich) for 7 hours and fixed immediately.

QUANTIFICATION AND STATISTICAL ANALYSIS

Phylogenetic Analysis

Genes were first identified by using annotated sequences from model organisms from major lineages for BLAST[92] into a custom local database of the *D. pealeii* transcriptome in Geneious. For top hits the entire sequence in the *D. pealeii* transcriptome was retrieved, the longest ORF was extracted and translated, then the amino acid sequence was trimmed for coding sequence. To find related sequences, BLASTp was used, searching both the Uniprot database in NCBI and retrieving only select vertebrate and *D. melanogaster* hits. BLASTp was performed again using the non-redundant protein database, and searching specifically for cephalopods, select mollusks, and *Limulus*. Trees that were not well resolved after these steps required an additional round of BLASTp, this time including more spiralian and ecdysozoan hits. Full sequences (or as long as is available) were aligned with our *D. pealeii* sequences for each tree using MAFFT v.7.450 in Geneious.[93] The only exception was our Sox tree where we used the alignment from,[99] which only included the HMG box of Sox proteins. This alignment focused on early metazoan species, so we added select vertebrates, mollusks, and ecdysozoans as described above, but trimmed sequences to include the HMG box for all. For all alignments we checked sequence redundancy and proper outgroups Fast Trees were made using FastTree2 v.2.1.11.[94] We constructed maximum-likelihood trees on the FASRC Cannon cluster supported by the FAS Division of Science Research Computing Groat Harvard University. We exported relaxed Phylip formatted alignment files and used IQ-TREE 2 v.2.1.0 with the following settings: iqtree2 -s ALIGNMENT.phy -st AA -nt AUTO -v -m TEST -bb 1000 -alrt 1000.[95] Unrooted trees were visualized as rooted by known outgroups and labeled by known annotated orthologues.

Imaging analysis

Image analysis was performed in Fiji.[35] Intensity range was adjusted in Fiji to better identify cell membranes. Drift correction was performed using Fiji plugin CoordinateShift (written by Housei Wada, https://signaling.riken.jp/en/en-tools/imagej/). Nuclear tracking was performed both manually and using Fiji plugin Trackmate.[35,83] Tracks were visualized and distance and velocity measurements were obtained from Trackmate and plotted graphically, normalizing to the highest point in migration. Image analysis for BrdU and PH3 was performed manually on central retinal sections of at least 3 embryos per time point and between 3-6 retinas. +/-SEM (standard error of the mean) was calculated and shown. Image analysis for PH3 in CytoD and Nocodazole treated embryos was performed manually on at least 3 embryos per treatment, with 4-6 central sections counted. +/- SEM was calculated and shown.

RNA-seq and Bioinformatics

Stage 23 embryos were treated with the gamma-secretase inhibitor DAPT at 20um in filter sterilized sea water for 24 hours and Control embryos were treated with the equivalent amount of DMSO, as previously described.[23] DAPT and Control eyes were dissected, pooled and macerated in TRIzol and stored at -80 degrees Celsius. RNA was extracted using a standard TRIzol (Invitrogen #15596026) chloroform extraction and passed through a gDNA eliminator mini-spin column (Qiagen #1030958). RNA was precipitated with isopropanol and then again precipitated with ethanol and checked for quality. Library prep and sequencing was performed at the Bauer Core at Harvard University. RNA-seq libraries were generated using the Kapa mRNA-Hyper Prep kit with Poly-A Selection (Roche, Basal) and were sequenced on the Illumina NovaSeq (>70 million 2x150 bp sequences) (Illumina, San Diego, CA).

Sequence quality control was performed according to the best practice recommendation on the Harvard FAS Informatics pipeline (https://informatics.fas.harvard.edu/best-practices -for-de-novo-transcriptome-assembly-with-trinity.html). Erroneous kmers were removed from the paired end Illumina dataset using rCorrector. Reads with Ns or other low complexity pairs were removed using a custom Python script provided by the Harvard Informatics GitHub (FilterUncorrectabledPEfastq.py). Adapters and low quality bases were removed using TrimGalore![84] Reads that mapped using Bowtie2 to the rRNA databases SILVA 132 SSURef Nr99 tax and SILVA 132 LSUParc tax were removed.[85] Pseudomapping was performed by Kallisto with 100 bootstraps to a previously published whole embryo transcriptome.[23,86] Transcript abundances were imported using tximport (https://bioconductor.org/packages/3.7/ b ioc/vignettes/tximport/inst/doc/tximport.html#use-with-downstream-bioconductor-dge-packages) into DESeq2 using the Kallisto abundance.h5 files. Differential gene expression was determined by importing transcript level abundances and gene level offset using *DESeqDataSetFromTximport*.[100] The DESeq2 pipeline was run and differentially expressed genes were considered with a p value of.05 and $\log_2$ fold change of above 1 and below -1 [97] (Table S1). All genes shown in the chord plots in Figure 4 meet these criteria with the exception of Notch which was included with a $\log_2$ fold change of -0.83. GO annotations were identified using the DAVID functional annotation tool.[88] Chord plots were generated using the R package GOPlot[89] and gplots.[90] The volcano plot was generated using VolcaNoseR.[91]

Current Biology, Volume *32*

Supplemental Information

Cephalopod retinal development shows vertebrate-like mechanisms of neurogenesis

Francesca R. Napoli, Christina M. Daly, Stephanie Neal, Kyle J. McCulloch, Alexandra R. Zaloga, Alicia Liu, and Kristen M. Koenig

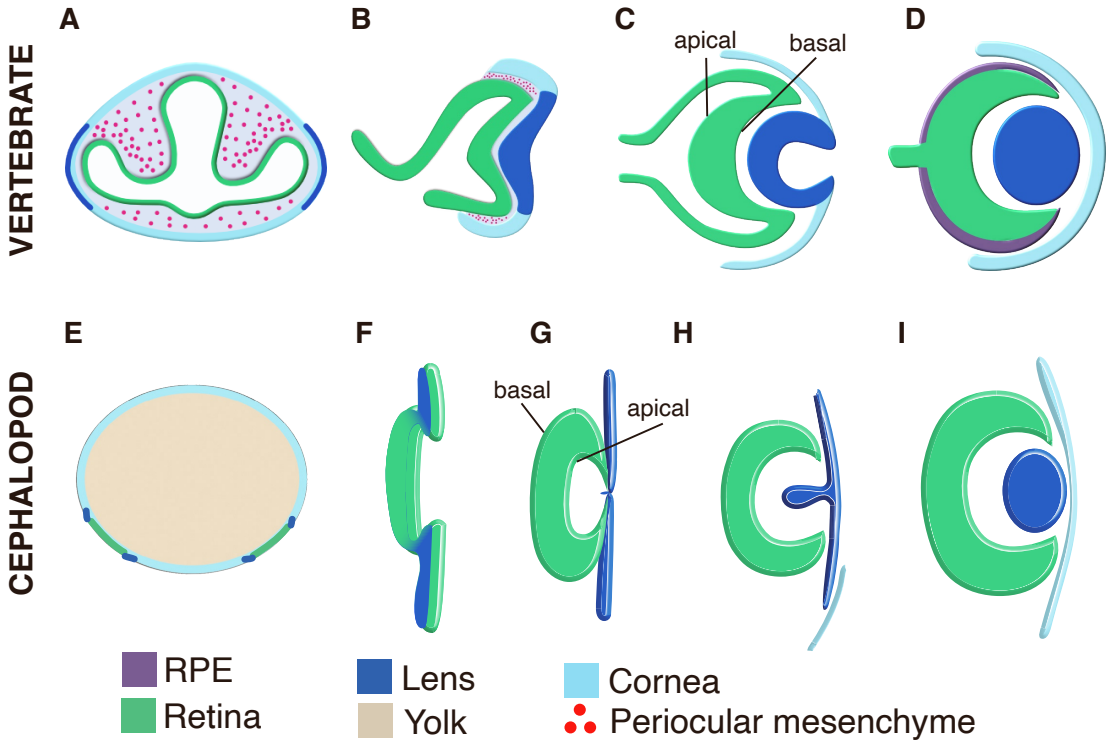

Figure S1: Summary figure of retinal epithelial morphogenesis in vertebrate and cephalopod development, Related to Figure 1. (A-D) Time course of retina morphogenesis in vertebrates. A) Coronal section. Vertebrate eye development begins with the evagination of forebrain early in development. **(B-D)** Retina cross section. **(B-D)** The retinal epithelium forms from and invagination of the evaginated forebrain tissue. **(E-I)** Time course of retina morphogenesis in cephalopods E) Arnold stage 19 embryo cross section.[S1] **(F-I)** Retinal cross section. **(F-G)** The retina placode is internalized and the eye vesical is formed. **(F)** Stage 19. G) Stage 23, **(H)** Stage 27, **(I)** Hatching. Apical and basal side of the epithelium is labelled in both the developing vertebrate and cephalopod retina.[S2]

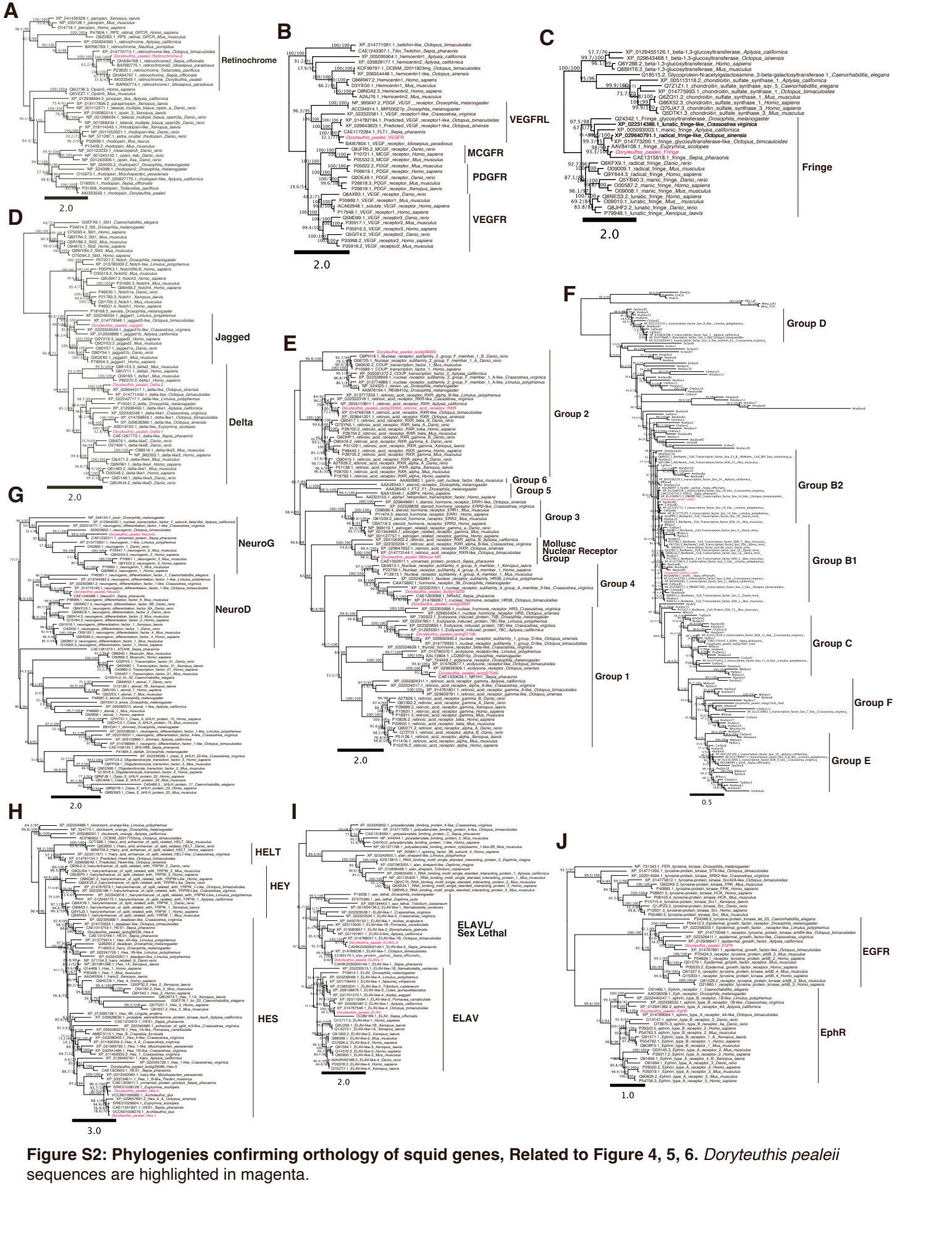

Figure S2: Phylogenies confirming orthology of squid genes, Related to Figure 4, 5, 6. *Doryteuthis pealeii* sequences are highlighted in magenta.

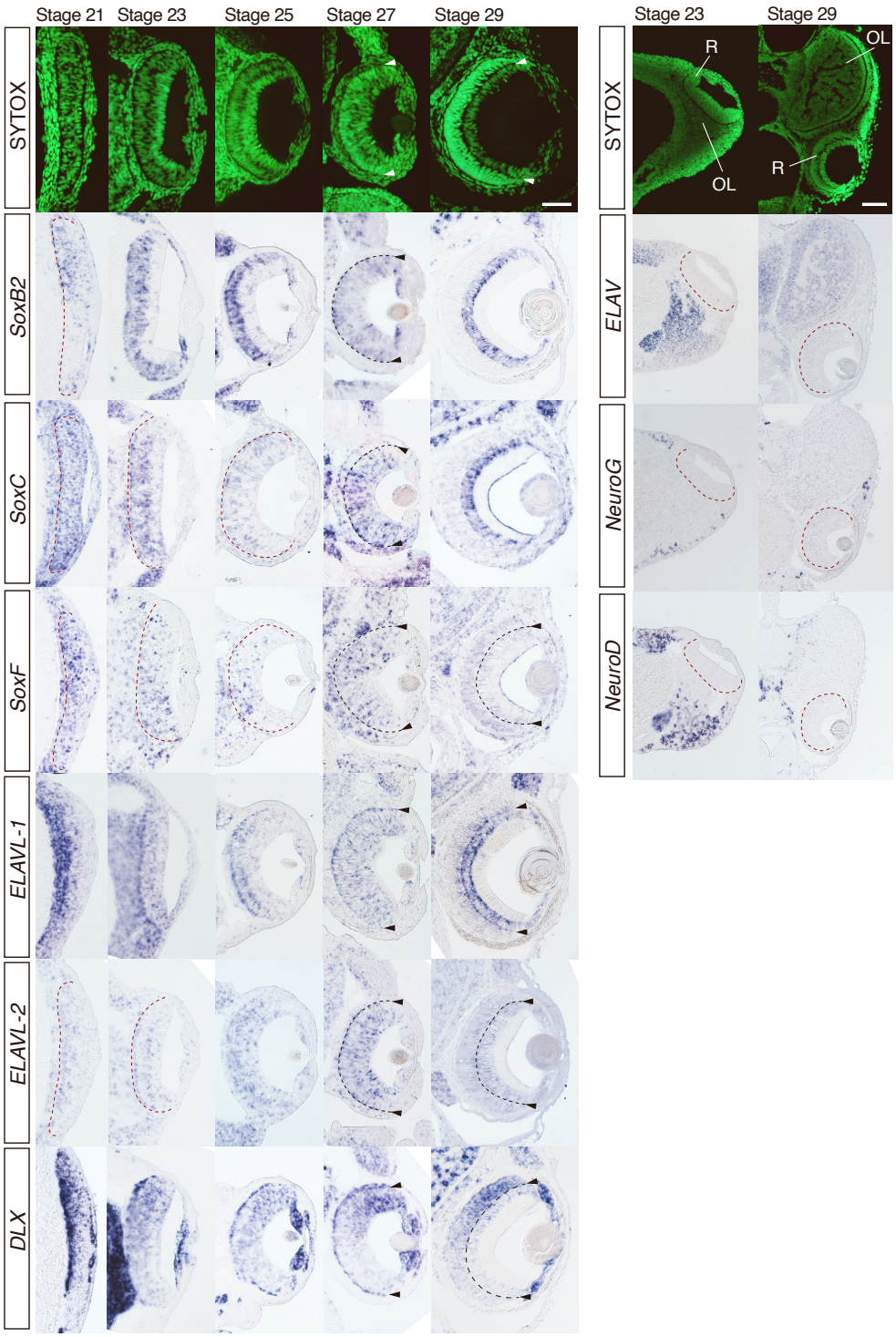

Figure S3. Canonical neurogenesis gene expression in the squid retina throughout development, Related to Figure 4. *DpSoxB2* stage 23-29 expression recapitulates *DpSoxB1* expression in the retina showing correlation with retinal progenitor cell expression. *DpSoxB2* Stage 21 expression differs from *DpSoxB1* showing a gradient of expression. *DpSoxC* and *DpSoxF* are both expressed in the developing retina throughout development. *DpSoxC* is specifically expressed in the support cell layer at Stage 29. Both *DpELAVL-1* and *DpELAVL-2* is expressed in the developing nervous system and the developing retina. *DpELAV-1* is expressed in the support cell layer and a population of cells posterior of the basal membrane similar to *DpEphR* expression. *DpDLX* expression maintains a gradient throughout development. *DpELAV, DpNeuroG, DpNeuroD* are all expressed in the developing nervous system but are excluded from retinal development. Nuclear SYTOX-Green shown in green. Red dotted lines identify the posterior retinal boundary. Arrowheads and the black dotted lines identify the basal membrane. Stage 21, 23, & 25 embryo anterior is down. Stage 27 & 29 embryo dorsal is up. *OL*: Optic Lobe; *R*: Retina. Scale is 50um.

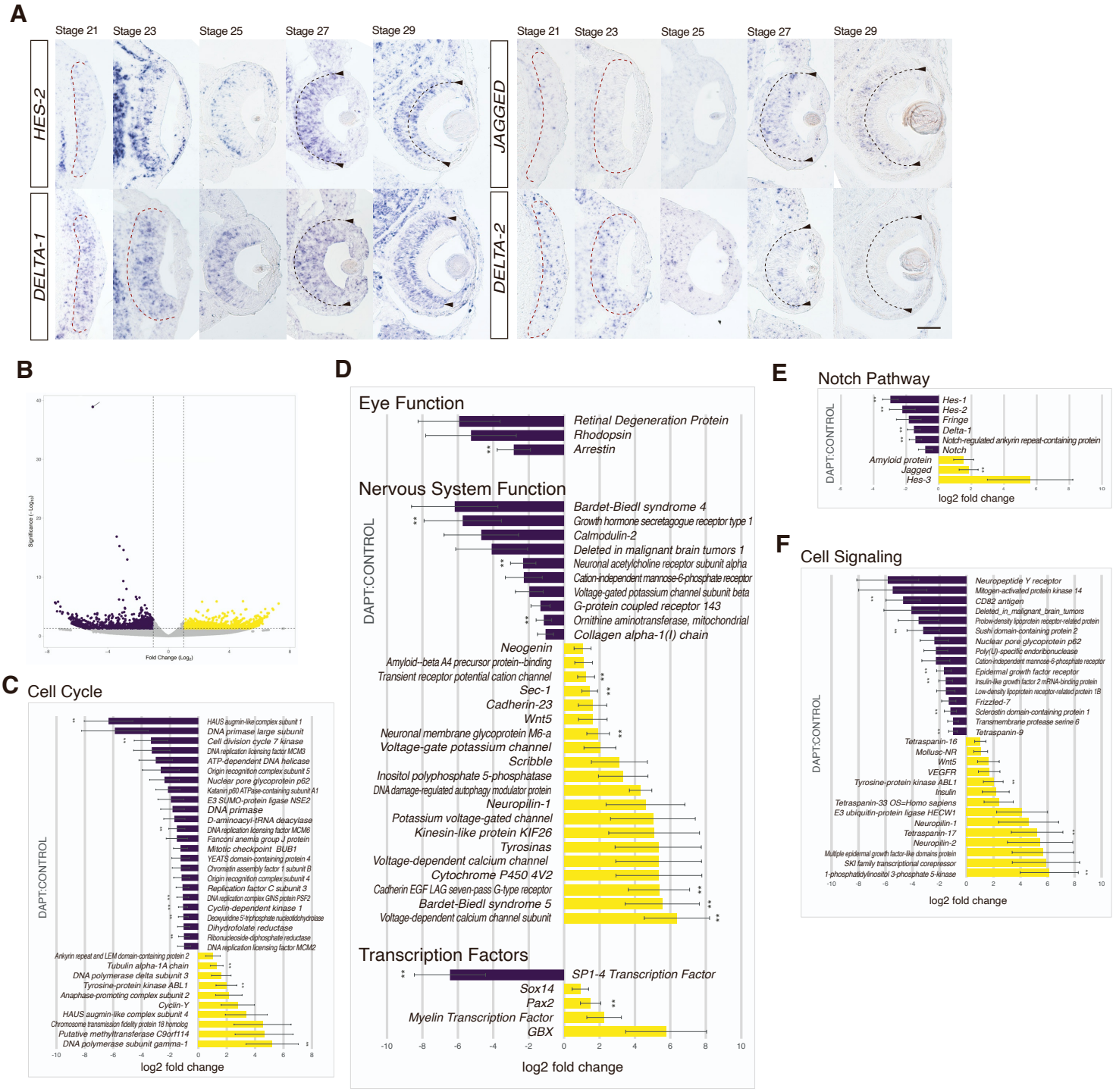

Figure S4. Notch signaling pathway expression and inhibitor RNA-seq analysis, Related to Figure 5. **(A)** *DpHes-2* shows expression at stage 23 correlated with retinal progenitor cell population. *DpHes-2* expression is enriched in the posterior at stage 25. *DpJagged* expression is found in the retina during development, although inconsistent across stages. *DpJagged* is clearly expressed at stage 27 and 29. *DpDelta-1* is uniformly expressed across the retina at all stages. *DpDelta-2* shows uniform expression across the retina from stage 21 to stage 27. *DpDelta-2* is not expressed at stage 29. Red dotted lines identify the posterior retinal boundary. Arrowheads and the black dotted lines identify the basal membrane. Scale 50um. **(B)** Volcano plot with differentially expressed genes highlighted in yellow and purple. Genes with differential expression of greater than log2 fold change of 1 and less than -1 with a p-value of less than .05 are highlighted. **(C-F)** Genes of note pulled out in respective groups. All genes shown have a p-value of less than .05 in the differential expression analysis. Those with a p-value of less than .01 are highlighted with **. Gene annotations are either best BLAST hit or the names given after phylogenetic analysis in this current investigation or previous publications.

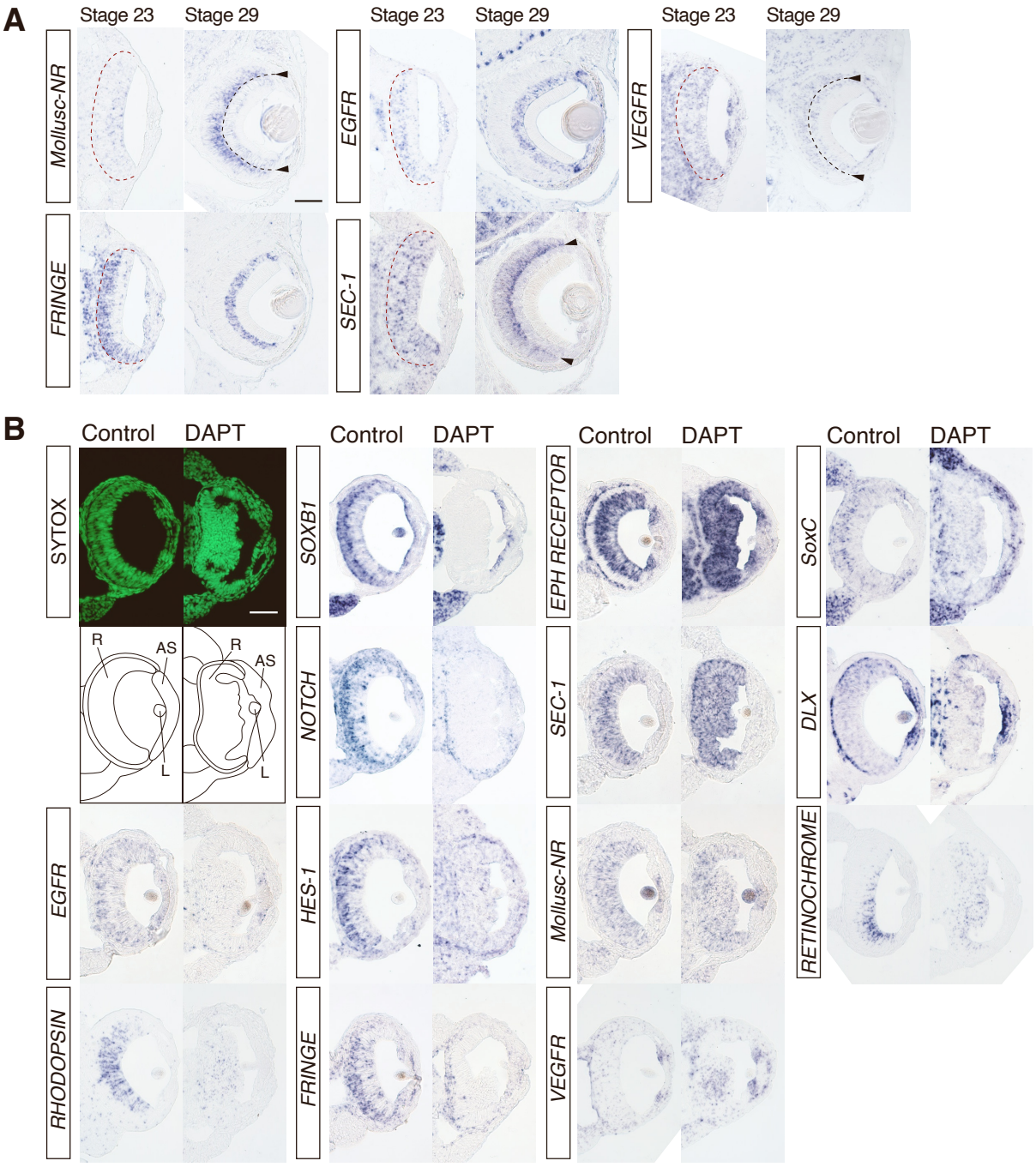

Figure S5. Wildtype expression at stage 23 and 29 of differentially expressed genes identified in DAPT:-Control RNA-seq experiment and DAPT and Control in situ hybridization studies, Related to Figure 5.
(A) Wild type *in situ* hybridization at stage 23 and stage 29 for genes differentially expressed in the retina after DAPT treatment. Stage 23 is at the time of treatment and stage 29 is at hatching. *DpMollusc-NR* is enriched in the anterior at stage 23 and posterior to the basal membrane at Stage 29. DpFringe, a part of the Notch signaling pathway, shows similar expression at stage 23 and 29 as *DpSoxB1*, *DpHes-1* and *DpNotch*, correlated with the retinal progenitor cell population. *DpVEGFR* is uniformly expressed in the retina at both stage 23 and stage 29. DpEGFR expression correlates with *DpSoxB1*. *DpSec-1* is uniformly expressed at stage 23 and enriched posterior of the basal membrane at Stage 29. Stage 23 embryo: anterior is down, stage 29 embryo: ventral is down. Red dotted lines identify the posterior retinal boundary. Arrowheads and the black dotted lines identify the basal membrane. **(B)** DAPT and Control gene expression. 20uM DAPT or DMSO treatments start at stage 23 and are treated with for 24 hours. Embryos fixed, wax embedded and *in situ* hybridization performed. Nuclear stain SYTOX-Green shown in green. Disorganization is apparent in DAPT treated retinas. Cartoon with label anatomy below. Data from Figure 5 included for comparison. *R*: Retina; *AS*: Anterior Segment; *L*: Lens. The first and second column show genes with decreased expression in DAPT-treated retinas. The third column are genes that show increased expression in DAPT-treated retinas. The fourth column show expression change outside the retina (*DpSoxC*) or genes showing similar expression (*DpDlx* and *DpRetinochrome*) in DAPT-treated embryos. Scale 50uM.

Gene Name	Forward Primer	Reverse Primer
Delta-1	AGGGTTTGGTGAACAGTCATCG	TGTCATTTAGGCTGGAAGGGC
Delta-2	CCCTTGGCAGTGTATCTGTGAAG	ACCAAGTTCCCCTGTTACGCAG
Jagged	TTTCTTTCCAGCAGTCACCA	CGGTTGGTTAGGAGTCTGAG
EGFR	CCATGAGAGTTGCTACCACA	GTATTTCGACCGCCAATGAC
EphR	TTTGATAGCCACGGTCATGR	GACAATCCACGAACTCCTCA
ELAV	CGGAAACAGCAATGAACACA	ACTCGTGTGCCAAGTAAGAA
ELAVL-1	TAACGGAACCTATTGCCTGG	TGGAGATTCTTGAGACTGCG
ELAVL-2	ATAACGGTAGCCATTCAGCC	RCAAGACAGAGCAACAGGTT
HES-1	GGAAAAACGCAGACGAACACG	GATGCTGTAAACGAAATCACCAGG
HES-2	CGTCTTCGTCAAAAACACAGGTC	GACAACCACCAAAACAGCATCTG
NeuroG	CGCTAGTTGTTTCGCCTTAC	CCCACTCCACTGTATCCATC
NeuroD	ACGTTGCTCTATCTTGTCCC	ACAGCTTCACCAATCCTCTC
Retinochrome	TGTCTGTGGAGTTGTGGTTT	TGCGTGTGGATTCTATGGTT
Rhodopsin	TCACGAGAAAGAGATGGCAG	GAGGGGGAGAGGAAAAGTTC
Sec-1	AGCTGTGAAGAAAAATGCCG	TACCCATAGCCAGATCCTGT
SoxB1	CACCATCAGTCGTTGTAGCGTG	GTGAAAAGCAGCCCAAAAAGG
SoxB2	AGAGTCCACCGTTAAGTTCG	TCCTCTCCAAAACGTGTACC
SoxC	TGCTTTTTGGTTCGCAACTCG	GGCAAGGTGATTTGATGAGGG
SoxF	TGGTGGGTCGGTCAACAGAATAG	CGGGCAATAGAATCATCGCAG
Mollusc-NR	TGACTCATCAAACGTGGGGT	ACTGAGTGTACGAAGGGCAG
EGFR	CCATGAGAGTTGCTACCACA	GTATTTCGACCGCCAATGAC
Fringe	GTCATTGAGCGTTGTAGGCC	AGACAGGGGTTTTATGGGGG
VEGFR	CAGTCATTGTTGGCAGTTCC	CATCCGTCGCATATAAGGGT

Table S2. Primer sequences for genes cloned in current study, Related to STAR methods

Supplemental References

S1 Arnold, J. M. (1965). NORMAL EMBRYONIC STAGES OF THE SQUID, LOLIGO PEALII (LESUEUR). In The Biological Bulletin (Vol. 128, Issue 1, pp. 24–32). https://doi.org/10.2307/1539386

S2 Koenig, K. M., & Gross, J. M. (2020). Evolution and development of complex eyes: a celebration of diversity. Development , 147(19). https://doi.org/10.1242/dev.182923